SYNTHESIS OF FLUORINATED SEGMENT CONTAINING OLIGOMERS FOR SUPERCRITICAL CARBON DIOXIDE APPLICATIONS

by

NALAN BİLGİN

Submitted to the Graduate School of Engineering and Natural Sciences
in partial fulfillment of
the requirements for the degree of
Master of Science

Sabancı University
Summer 2003

SYNTHESIS OF FLUORINATED SEGMENT CONTAINING OLIGOMERS FOR SUPERCRITICAL CARBON DIOXIDE APPLICATIONS

APPROVED BY

Assoc. Prof. Yusuf Menceloğlu ……..
(Thesis Supervisor)

Assoc. Prof. Canan Baysal ……..

Prof. Nihan Nugay ……..

DATE OF APPROVAL: …….

to my parents

&

my sister

ACKNOWLEDGMENTS

Writing this thesis took significant time away from my other responsibilities to instructors, friends, and family. First I would like to express my endless thanks to my advisor Yusuf Menceloğlu. I am indebted to him for his guidance, encouragement, and patience throughout the research and writing this work. I would also thank to Alpay Taralp for his help during the planning stages of the experiments.

Also special thanks to Burçin Yıldız for her assistance in teaching me to use and learn NMR for the characterizations of synthesized materials. I would like to thank Mustafa Demir, Çınar Öncel, Kazım Acatay, Mesut Ünal, and İstem Özen for their friendship and endless support.

Finally, my appreciation and gratitude go to my parents and my sister (Leman) for their valuable help and assistance during my 2-years at Sabancı University.

SYNTHESIS OF FLUORINATED SEGMENT CONTAINING OLIGOMERS FOR SUPERCRITICAL CARBON DIOXIDE APPLICATIONS

ABSTRACT

Two types of fluorinated block containing oligomers were synthesized and utilized as surfactant systems for supercritical carbon dioxide (CO_2) applications. Solubility experiments with the prepared oligomers were performed using a pressure-temperature controllable supercritical CO_2 device.

The experiment was designed in three steps. First, acylchloride ended di-functional azo initiator was synthesized from its acidic derivative. Then two types of fluorinated azo initiators were synthesized by esterification of the acylchloride groups through the reaction with two different fluoroalcohols in the presence of phase catalyst. The fluoroalcohols differed mainly in their end group character: While one's end group carbon was completely fluorinated, the other contained an extra hydrogen atom in this group.

The final and the main step of the experiment consisted of the synthesis of fluorinated tri-block oligomers. Several commercially available monomers were reacted with the fluoroinitiators through radical polymerization mechanism. With the two types of initiators two sets of oligomers were obtained. The obtained oligomer blocks were tri-blocks consisting of monomer repeating groups with fluorinated side segments.

Materials were characterized with infrared spectroscopy (FT-IR), nuclear magnetic resonance spectroscopy (^{1}H NMR, C^{13} NMR, and F^{19} NMR), and thermal analyses (DSC, TG/DTA)

Solubilities of the two oligomer series were tested in supercritical CO_2. The effects of end group nature, chain fluorination degree and chemical structure (intermolecular interactions) on solubility efficiency were investigated. Solubility is largely affected by the end group nature of the fluorinated segments and the intermolecular interactions occurring between the oligomers and the supercritical phase. Initial findings will be studied in details.

ÖZET

İki farklı tip, florlanmış grup içeren tri-blok oligomeri sentezlenmiş ve superkritik karbon dioksit (CO_2) davranışları incelenmiştir. Malzemelerin CO_2 çözünürlük testleri basınç-sıcaklık kontrollü süperkritik cihazıyla yapılmıştır.

Deney üç adımda tasarlanmıştır. İlk adımda azo bis siyano valerik asitten (ABCVA), karbonil-klorlu türevi sentezlenmiştir. Daha sonra, elde edilen madde iki çeşit floroalkolle esterifike edilerek florlu azo başlatıları sentezlenmiştir. Kullanılan alkollerin arasındaki en belirgin fark birinin zincirindeki son grupta ekstra hidrojen atomu bulunmasıdır.

Deneyin son ve en önemli adımında, ticari monomerler kullanılarak daha önce sentezlenen florlu azo baştatıcılarıyla florlu oligomerler sentezlenmiştir. İki çeşit başlatıcıyla iki grup oligomer elde edilmiştir. Elde edilen malzemeler tekrar eden monomer birimleri ve florlu yan gruplardan oluşan tri-bloklardır.

Malzemelerin karakterizasyonunda, infrared spektroskopi (FT-IR), nükleer manyetik rezonans spektoskopi (^{1}H NMR, C^{13} NMR, ve F^{19} NMR) ve termal analizler (DSC, TG/DTA) kullanılmıştır.

Elde edilen iki setin superkritik CO_2 çözünürlükleri test edilmiştir. Zincirlerin son grubundaki hidrojen atomu varlığının, zincirin toplam florlandırılmış yüzdesinin ve malzemelerin kimyasal yapılarının çözünürlük üzerindeki etkileri araştırılmıştır. Deney sonucunda, flor bloklarının son grubundaki hidrojen atomu varlığının ve malzemelerin kimyasal yapılarının çözünürlüğü önemli miktarda etkilediği anlaşılmıştır.

TABLE OF CONTENTS

LIST OF FIGURES

LIST OF TABLES

CHAPTER 1

INTRODUCTION

1.1. Supercritical Fluids

1.1.1. Brief Background on Supercritical Fluids (SCFs)

The supercritical state was first discovered by the French scientist, Baron Charles Cagniard de la Tour, in 1821. However, intensive research in the area actually belongs to the last few decades. Initially SCFs were utilized in the chromatographic separation and extraction separation processes. One important example to SCF extraction process is the caffeine extraction from coffee with $scCO_2$. Similarly the process has been expanded to different extraction applications with products such as tea, and spices. Recently, SCFs have been used as reaction media due to discovered benefits of their special properties.[1] SCFs have also found great interest in the area of polymer synthesis and processing. [2]

1.1.2. Definition and Properties

The supercritical phase of a compound is a phase in which the compound is above the critical points (critical pressure P_c, and critical temperature T_c) and below the solid state. In this phase, a compound bears both the properties of a gas and a liquid. The most important property of a supercritical fluid is its tunability in the temperature range since a small

change in temperature will cause drastic changes in the pressure, followed by changes in other physical variables related to pressure and temperature.

The main variables that are affected by such changes and that play important roles in supercritical applications are the density (d) and the dielectric constant (ε). The density is a variable known to be directly proportional to the solvency power, and this is the basis for supercritical fluid extraction processes. The tunability of the dielectric constant also gives power to tune the solvency power, since it relates to the solvent polarity and other important solvent effects.

Supercritical fluids have many important properties that increase their attractiveness for use. Their high diffusivity, low viscosity and high density make them suitable for continuous-flow processes. Another asset of supercritical fluids is that they have tunable solvating power (indicated in the beginning of section 1.1.2). In this way, different conditions may be set for a wide range of applications concerning different compounds. Also, supercritical fluids are volatile compounds, which can be easily removed after usage, avoiding any solvent wastes and costly separations. Even though the costs of the equipment needed to run a supercritical process are high, they are generally outweighed by the economic benefits brought by SCF applied processes.[3] Figure 1.1 illustrates a general pressure-temperature phase diagram for a pure compound. The supercritical phase and the pressure-temperature range defining this phase are shown on the figure.

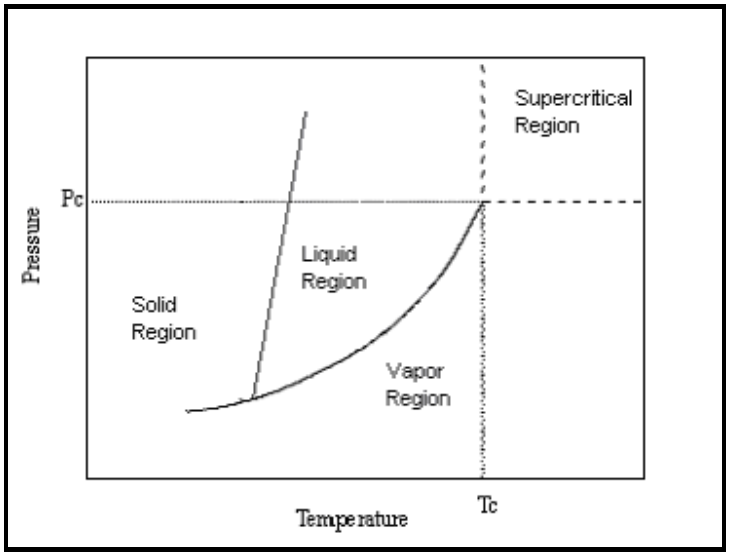

Figure 1.1. Basic temperature-pressure phase diagram for a pure substance[4]

Important supercritical properties can be summarized under the following items:

i. A SCF is a substance under pressure above its critical temperature.
ii. Under these conditions the division between gas and liquid does not apply and substance can only be described as a fluid.
iii. SCFs have physical intermediate properties to those of gases and liquids, and these properties are controlled by the pressure.
iv. SCFs do not condense or evaporate to form a liquid or a gas. Compounds like supercritical xenon, ethane and carbon dioxide afford a wide range of uncommon chemical opportunities in both synthetic and analytical chemistry.
v. As the density increases, solubility increases too (i.e. with increasing pressure). Fast expansion of supercritical solutions leads to precipitation of a finely divided solid.
vi. The fluids are completely miscible with permanent gases (e.g. N_2 or H_2) and this leads to much higher concentrations of dissolved gases than can be achieved in conventional solvents. This effect adds benefit in the applications with organometallic reactions and hydrogenation.

1.1.3. Solubility in a SCF

According to the ideal gas law, solubility (γ) is the ratio of vapor pressure (p_v) to total pressure (p_t). In a SCF, however, the behavior is nonideal and the solubility raises several orders of magnitude. The reason for this increase in the solubility is due to the increase in the density of the SCF. Increase in solubility is defined by the enhancement factor (E) that is merely the ratio of the actual solubility to the one predicted by the ideal gas law.

$$(E) = \gamma.p_t/p_v \tag{1.1}$$

Solubility for a given solute also depends on the SCF itself. Different supercritical fluids have different solubilising efficiencies. This difference arises due to various intermolecular interactions occurring between the solvent and the solute, which can be explained by the solvent polarity. Here the ‘’like dissolves like’’ rule applies. Thus a polar

solvent is expected to dissolve a polar solute more efficiently than a non-polar one. In the same way, the structure similarity of both the solvent and the solute plays a role in the solubility efficiency.

1.1.3.1. Temperature and Pressure Effect on Solubility

Basically, solubility is directly proportional to pressure; that is to say, the higher the pressure, the higher the dissolving power of the supercritical fluid.

Figure 1.2 shows the solubility of naphthalene in $scCO_2$. Solubility increases initially and gets almost constant after approximately 250 atm. This behavior represents the density changes occurring in the solvent.

The effect of temperature on solubility is more complex, though. The solubility of a certain solute depends both on its vapor pressure and on the density of the solvent. The temperature dependence of both variables causes the crossover effect on the solubility of the solute. The intersection of the isotherms of a given solute at a pressure-solubility diagram gives the crossover pressure. The region below the crossover pressure is the retrograde region. In this zone, any increase in temperature causes the density to fall, in turn decreasing the solubility. At any pressure greater than the crossover value, the effect of temperature on density is not very high and the dominant effect is caused by the vapor pressure of the solute. Temperature increase in this region increases the vapor pressure, which in turn results in enhanced solubility.[5] The crossover effect is represented in Figure 1.3 for naphthalene in supercritical carbon dioxide. Figure 1.3 illustrates the dependence of supercritical mixture solubility on the solute vapor pressure and fluid density.

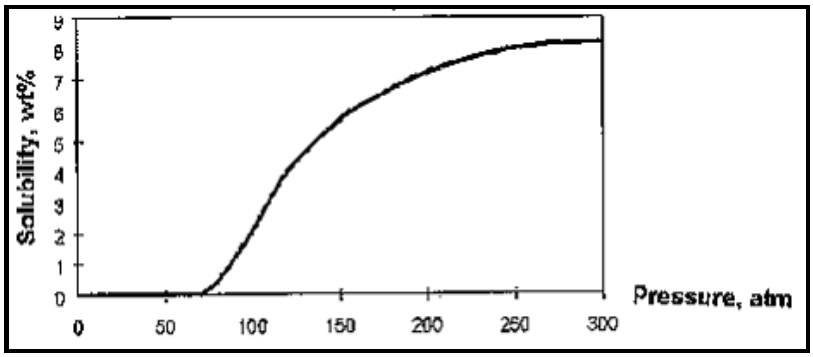

Figure 1.2. Solubility of naphthalene in supercritical carbon dioxide (45 °C)[6]

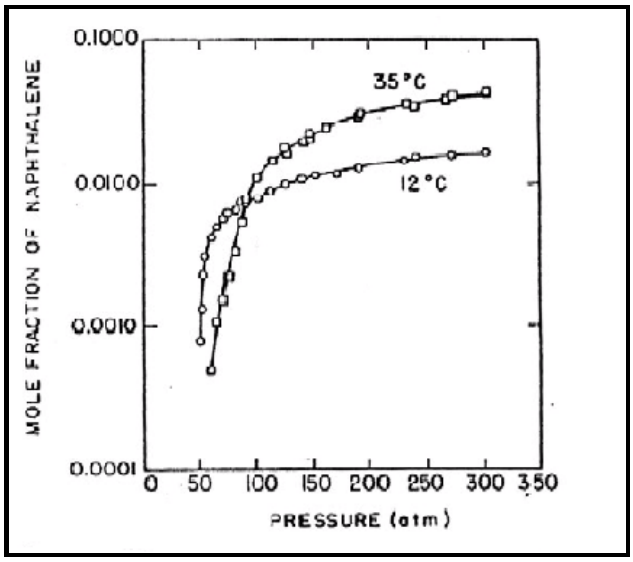

Figure 1.3. The solubility of naphthalene in supercritical ethylene, showing the crossover effect [7]

1.1.4. Supercritical Carbon Dioxide ($ScCO_2$)

Having several important environmental, chemical, process, health and safety advantages, $scCO_2$ is the most widely exploited SCF fluid. These properties were explained in much detail for SCF fluids in the previous section. Most important properties of $scCO_2$ are summarized in Table 1.1.[8]

Table 1.1. Benefits of $scCO_2$ as an industrial solvent

Environmental Benefits	**Health and Safety Benefits**	**Chemical Benefits**	**Process Benefits**
Does not contribute to smog	Non-carcinogenic	High miscibility with gases	No solvent residues
Does not damage ozone layer	Non-toxic	Altered cage strength	Facile separation of products
No acute ecotoxicity	Non-flammable	Variable dielectric constant	High diffusion rates
No liquid waste		High compressibility	Low viscosity
		Local density augmentation	Adjustable solvent power
		High diffusion rate	Adjustable density
			Inexpensive

Table 1.2 describes the variations between some basic parameters defining physical phase properties.[8] The density of $scCO_2$ is approximately 0.4 g/cm^3. Due to the liquid-like density of $scCO_2$, many compounds dissolve at degrees higher than the ones predicted by the ideal gas formulations. Since the solvating power of a SCF is directly proportional to its density, varying the temperature and pressure will make it possible to tune the density and thus control the solubility and separation of a specific material.[4] Table 1.3 illustrates some commonly used supercritical fluids together with their critical temperatures and pressures.

Table 1.2. Comparison of the general properties of liquid, gas and $scCO_2$[9]

Phase	***Density, (g/cm^3)***	***Diffusion Coefficient, (cm^2/s)***	***Viscosity, (poice) (g/cm.s)***	***Surface Tension, (dynes/cm)***
Liquid	1	10^{-6}	10^{-2}	45-60
Supercritical Fluid	0.2-0.8	10^{-3}	10^{-3}	0
Gas	0.001	10^{-1}	10^{-4}	N/a

Table 1.3. Critical conditions for various supercritical solvents[10]

Fluid	Critical Temperature (K)	Critical Pressure (bar)
Carbon dioxide	304.1	73.8
Ethane	305.4	48.8
Ethylene	282.4	50.4
Propane	369.8	42.5
Propylene	364.9	46.0
Fluoroform	299.3	48.6
Ammonia	405.5	113.5
Water	647.3	221.2
n-Pentane	469.7	33.7

The solubility efficiency is closely related to the transport properties of a solvent. These properties are defined by the diffusion coefficient and the viscosity. When compared with those of liquid solvents, the diffusion coefficient (diffusivity) and viscosity of SCFs are several magnitudes higher and lower, respectively. Then the rate of diffusion of the species in a SCF will be faster than in a liquid solvent; this faster rate will directly contribute to a more efficient solubility in a SCF. Just as the density is affected by pressure changes, the diffusion coefficient also varies with changes in the pressure and temperature, and at the same time is affected by the change in the density and the viscosity.[5]

$ScCO_2$'s critical temperature below 35°C enables work at moderate temperatures; thus, $scCO_2$ is more convenient for processes carried out with thermally unstable materials. In addition, removal of the supercritical solvent by simply releasing the pressure eliminates the costly solvent separations and provides solvent free high purity products. $ScCO_2$ processes are also very important environmentally.

1.1.4.1. Difficulties and Drawbacks of $ScCO_2$

In the compressed phase, $scCO_2$ has a low dielectric constant and a very low polarizability. The result of these two properties is the reduced ability for formation of sufficiently strong van der Waals interactions between the solvent and the solute.[11] Thus $scCO_2$ is a poor solvent for most of the non-polar compounds and for most of the polar non-volatile compounds. Likewise, most of the polymers having high molecular mass are not soluble in $scCO_2$. The known exceptions are poly(ether-carbonates),[12] fluorinated polymers and silicone based polymers. Figure 1.4 illustrates the categorization of the solubility of polymeric materials in $scCO_2$. These molecules have low cohesive energy density and low surface tension, which give them the relatively higher solubility efficiency.[1] Table 1.4 summarizes the main properties of $scCO_2$ that cause problems and difficulties when dealing with $scCO_2$ applications.

Table 1.4. Drawbacks and difficulties of CO_2[8]

Difficulties	**Drawbacks**
Low dielectric constant	Capital cost of liquid pressure equipment
Low polarizability per volume	Lack of enough operation plants
Neither liphophylic, nor hydrophilic	Lack of innovative unit-operations to reduce utility consumption
	Understanding nature of reactions and solvency properties

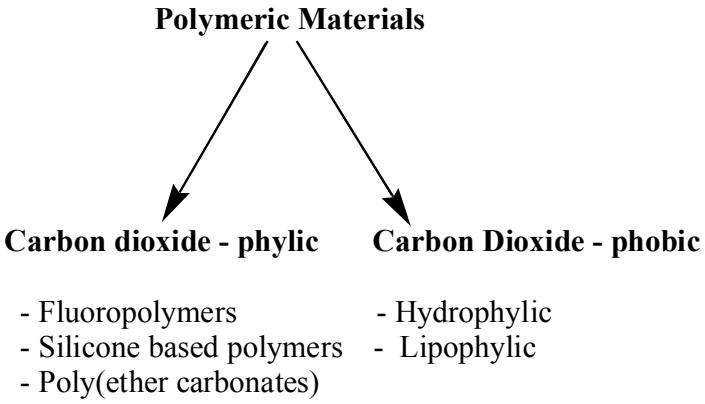

Figure 1.4. Solubility of Polymeric Materials in $scCO_2$

1.1.4.2. The importance of $ScCO_2$ for Present Applications

$ScCO_2$ can be utilized as a continuous phase in a very wide range of applications such as emulsion polymerization, chromatography of highly polar compounds, heavy metal decontamination in wastewater, advanced oil recovery techniques, and preservative transport into a permeable medium.[13] Some other important applications that can be carried out in $scCO_2$ are microelectronics manufacturing, textile dyeing, and preparation of nanoparticles, enzymatic reactions and natural product extractions. In all these areas, as mentioned previously, the main problem faced is the low solubility efficiency of CO_2.

Even though CO_2 lacks a dipole moment, which is the main reason for solubility problems, its large quadrupole moment contributes to its solubility parameter. This property coupled with the Lewis acidity of the CO_2 is the basic starting point for research to design CO_2 compatible materials. Thus, the design of new compounds that will serve as carriers between immiscible systems (surfactants) is of great importance.[14]

The scope of this work is to design and synthesize new surfactants for the SCF application of CO_2, mainly in polymer synthesis and processing. Almost any polymer applications such as synthesis, and processing occur at elevated pressures. Polymerizations naturally occur above the critical point. Utilization of SCFs enables the control of conditions by temperature-pressure modulation. The high diffusivity of supercritical fluids

makes them better penetrating solvents and thus they are more efficient in residual removal than alternative liquid organic solvents.[9]

1.2. Surfactant Systems

1.2.1. Basic Information

Microemulsions are a thermodynamically stable system that consists of at least three components: Two immiscible components and a carrier surfactant component.[15]

Surfactants are amphiphilic-emulsifying agents, which are chain molecules composed of hydrophobic or "tail" parts and hydrophilic or "head" parts. A basic amphiphile forms aggregates in water or in the solvent of the specific application. The aggregate formation is due to the fact that the tail parts of the amphiphile are hydrophobic and repel the water molecules (for water system), while the head parts are hydrophilic and do not. When allowed to move freely, the chain molecules form clusters with the tails in the center of the cluster.

The concentration and size of these aggregates depend mainly on amphiphile structure, and concentration. The main factor affecting the size of the clusters is the number of tail segments in the amphiphiles. However, contrary to expectation, the size of the aggregates does not significantly change with amphiphile concentration. There is a concentration below which micelles do not form. This concentration is called the critical micelle concentration (CMC). Below this concentration, the system mainly consists of monomers and small groups of amphiphiles. CMC is a measure of the free energy of the micelle formation of the system. The lower is the CMC, the more stable are the formed micelles and the more slowly are they embedded into or rooted out from the micelle. The average number of monomers in a micelle is assigned as AN. CMC and AN are strongly affected by temperature. When the temperature is low, surfactants form a cloudy crystalline suspension. If the temperature is increased, these crystals dissolve to form monomers if the concentration is below the CMC or form micelles if the concentration is above the CMC.

The temperature at which micelle formation is observed first is called the critical micelle temperature (CMT). There is an equilibrium point, called the Krafft Point, at which crystals, monomers, and micelles exist in equilibrium.[16]

The hydrophilic groups give the primary classification to surfactants, and are anionic, cationic and non-ionic in nature. The surfactant molecules align themselves at the surface and internally so that the hydrophile end is toward the water and the hydrophobe are squeezed away from the water. Figure 1.5 represents a simple sketch of the event.

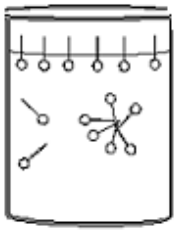

Figure 1.5. Schematic sketch of surfactant molecules in water

Due to their typical behavior to orient at surfaces and to form micelles, all surfactants perform certain basic functions. Selection of surfactants, orders of addition and relative amounts of the two phases determine the class of emulsion.

One other important function is solubilisation, which is closely related to emulsification.[17] As the size of the emulsified droplet decreases, a condition is reached where this droplet and the surfactant micelle are the same size. At this stage, an oil droplet can be imagined as being in solution in the hydrophobic tails of the surfactant and the term solubilisation is used. Emulsions are milky in appearance and for example solubilised oils appear clear to the eye.

1.2.2. Fluorinated Surfactants and Micelle formation in $ScCO_2$

There are several known functional groups that interact favorably with carbon dioxide. All of these have low solubility parameter like carbon dioxide itself, thus they are

expected to be soluble in CO_2. Table 1.5 displays these functional groups together with their special parameters leading to good solubility.

Table 1.5. Functional groups that interact favorably with carbon dioxide[13]

Functional Group	Property Leading to Favorable Interaction
Dimethyl Siloxane	Low solubility parameter, (4-7.5(cal/cm^3)$^{0.5}$)
Hexafluoropropylene Oxide	Low solubility parameter, (4-7.5(cal/cm^3)$^{0.5}$)
Fluoroalkyl	Low solubility parameter and low dipolarity/polarizability parameter (-0.5-0.0)
Tertiary Amines	Lewis Base
Aliphatic Ethers	Lewis Base
Aliphatic Esters	Lewis Base

Major work dealing with the problem of solubility in SCF are concentrated on the synthesis of fluorinated oligomers that will act as an intermediate carrier, in other words as a surfactant, between the SCF and the reactants. This idea is simply based on the fact of micoemulsion formation in compressible fluids.

Several investigators have dealt with the problem of solubility and have reported that due to the low (less than zero) polarizability/dipolarity parameters of scCO_2 and perfluorinated alkanes, fluorination of a certain compound leads to improved CO_2 solubility. Perfluoroalkyl polyethers have a solubility parameter of 4-5 (cal/cm^3)$^{0.5}$ and carbon dioxide has a solubility parameter of 5.5-6 (cal/cm^3)$^{0.5}$ at 293K over the 800-900 kg/m^3 range. Thus these are expected to be miscible with each other. Among the commercially available surfactants, the fluorinated ones dissolved at lower pressures inscCO_2 when compared with other halogenated analogues. Important factor that accounts for the improved solubility of fluorinated compound in CO_2 is the etheric oxygen atom of the fluorinated tail of the surfactant. Being a weak Lewis acid, this oxygen has an electron donor capacity and enhances the miscibility with carbon dioxide.[13]

The designed fluorinated copolymer consists of two blocks: one being the CO_2-philic block and the other one being the CO_2-phobic block. The surfactant forms micelles with the CO_2-phobic head in the core. With the relation to the oil-in-water system, these micelles are

referred as inverse micelles. When the density of CO_2 is increased, the solvation of the two components of the diblock copolymer increases too and the result is a decrease in aggregation and finally formation of unimers. Then the existence of a critical micelle density (CMD) is expected and it is similar to CMC observed in aqueous media.[18]

The surfactants used in $scCO_2$ contain fluorinated tails. The fluorine atom is a large sized highly electronegative atom, which brings quite different properties to the surfactant. If the analysis is done at the molecular scale, the strong attractive interactions between the solvent molecules' quadrupoles and multipoles caused by fluorinated compounds can be shown as the main reason for the high solubility.[19]

Being large sized, fluorine atoms add bulkiness to the chain, which makes the chain more rigid than the hydrogenated analog. The effect is observed as a diminished surface curvature of the chain. This is the reason why the aggregates that are formed in solution are larger in size when compared to their hydrogenated correspondents.

1.3. Research Objectives

Beckman and his group designed the first supercritical CO_2 effective surfactants.[20] These were mainly fluorinated hydrocarbons. Different kinds of surfactants were synthesized according to their application area. These include surfactants designed for water-in-carbon dioxide (w/c) systems,[21] perfluoropolyether (PFPE),[22] [23] [24] and similar fluorine based compounds and mixtures of different surfactant systems.

The importance of finding an appropriate surfactant for a specific system is obvious. Yet, for a specific application, the scientist's or the industrialist's main concern is to find the most efficient material for the desired conditions. Then, by combining the properties leading to good CO_2 solubility, it is possible to design a surfactant with optimum solubility efficiency.

In this work, the aim is to synthesize surfactants that will be active in both carbon dioxide phase and in organic phase. The functional groups compatible with CO_2 were stated previously. Combining these and the knowledge obtained from previous studies, we deal

with the problem of obtaining a satisfyingly efficient surfactant with the commercially available several monomers and two types of alcohols. The effect of etheric oxygen as a Lewis base and fluoroalkyl type compounds' CO_2 compatibility were discussed previously. CO_2 itself acts as a Lewis acid when other electron donor groups are present in the system.[25] Thus an etheric group is expected to be carbon dioxide compatible. Fluoroalkyl groups are also compatible due to their low solubility parameters and low dipolarity/polarizability parameters.

In this work, the designed surfactant is a block type oligomer with fluorinated side alkyl groups connected to a hydrocarbon chain by an ester group. The synthesis is achieved through the reaction of several available monomers with two-side fluorine segment containing azo-type precursors (initiator) synthesized by reacting fluorinated alcohols and again previously obtained carbonyl chloride di-functional azo type compounds. The main differences between the two surfactants are the dergree of fluorination on the side chains and side chains' end group character. By end group character, we mean the availability of a hydrogen atom on this group. The effect of this hydrogen was also discussed by Eastoe et al.[26]

In summary, this work deals with the synthesis of specific supercritical applicable surfactants to solve the solubility problem by comparing the two main effects on the solubility efficiency and aims to determine most suitable experimental conditions required. Throughout the research, calculational studies performed by Kirmizialtin et al. are also used as a theoretical basis. They have performed single chain molecular dynamics simulations to understand the dynamic and conformational behavior of various ethylene type monomers in $scCO_2$. The work showed that the van der Waals forces were the dominant intermolecular interactions that determined oligomer behavior in supercritical phase. [11]

CHAPTER 2

SYNTHESIS OF FLUORINATED AZO INITIATORS

2.1. Introduction

As mentioned previously, the design of supercritical carbon dioxide ($scCO_2$) active surfactants is an important issue to solve the problem of CO_2 solubility and make benefit of the wide range of supercritical advantages. This chapter explains the synthesis of two fluorinated azo type free radical initiators to be used in fluorinated oligomer synthesis.

The first step of the synthetic procedure is the chlorination reaction of 4,4'-Azobis (4-cyanovaleric acid) (ABCVA). Before carrying out the reaction, separating the two isomers of 4,4'-Azobis (4-cyanovaleric acid), the trans isomer and the cis isomer, is an important step that must be carried out to obtain higher conversions in the further chlorination reaction of the acid. This is because each isomer has different reactivity towards chlorination.

The difference in the reactivity of the two isomers can be explained by steric hindrance. The trans isomer sterically more hindered, and thus the carbon of the carbonyl group is less available to a nucleophilic attack.[27]

Reacting the acid without isomer separation and allowing the reaction to continue for longer duration in order to ensure the complete conversion of the trans isomer is in the expense of the cis isomer decomposition. The acid itself is a free radical initiator and is

sensitive to high temperatures as well as light. On the other hand, if the reaction is kept shorter to prevent decomposition, the total conversion of the trans isomer is not possible and this time impurity of a non-reacted acid forms. Therefore, separation of the isomers is crucible.

The isomers show different solubility patterns in ethanol and this is the basic idea used for isomer separation. The cis isomer is quite soluble in ethanol, while the trans isomer is not.[28]

The second step is the chlorination reaction. There are several known basic ways to chlorinate an acid group. A carboxylic acid can be transformed into an acyl chloride by reacting it with thionyl chloride ($SOCl_2$) or with phosphorous trichloride (PCl_2) while applying heat during the reaction.[29] In this experiment thionyl chloride is utilized for the chlorination reaction.[30] Figure 2.1 illustrates the chlorination reaction by which the acid (ABCVA) is converted to ABCVCl.

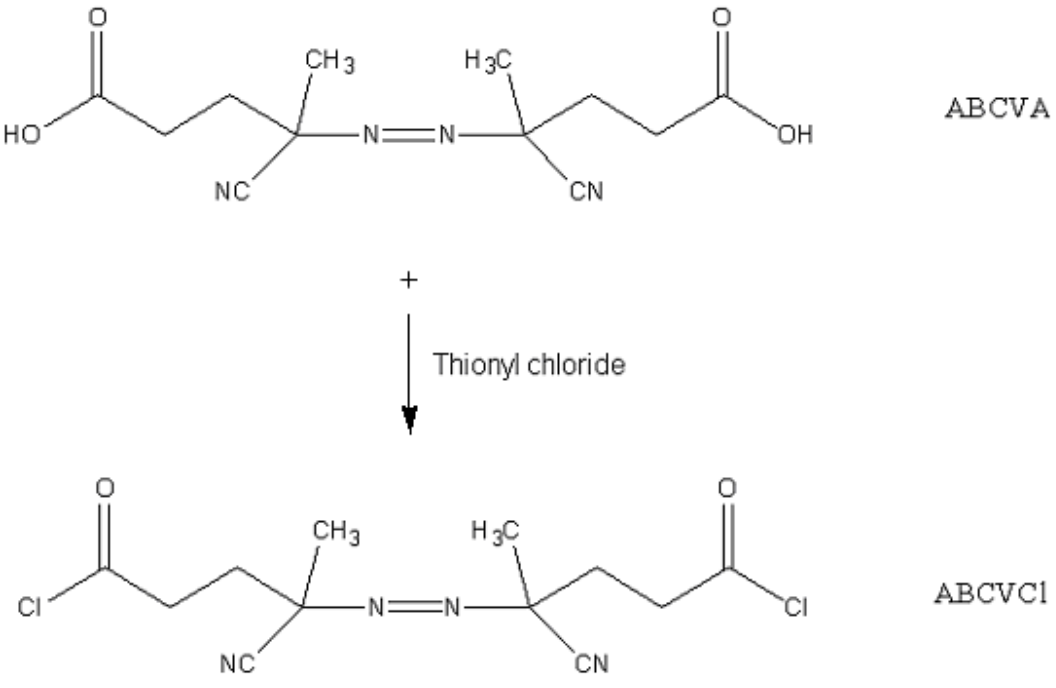

Figure 2.1. Schematic representation of the chlorination reaction of carboxylic acid groups with thionyl chloride

In the final step, esterification of the side-chlorinated carbonyl groups is achieved. The esterification is a condensation reaction carried out by reacting a hydroxyl group and an acyl chloride group. A condensation reaction yields a small molecule, which is a hydrochloric acid (HCl) molecule in this experiment. The reaction proceeds easily at room temperature with a small amount of phase transfer catalyst added. The esterification reaction of ABCVCl is illustrated by Figure 2.2. The addition of fluorinated chains proceeds from both sides of the molecule and acyl chlorides are replaced with ester groups.

Two different initiators are synthesized using two different alcohols. Their functioning will be analyzed in the next chapter that deals mainly with the oligomer synthesis and $scCO_2$ solubility. The effect of utilizing different initiators on the fluorination degree of an oligomer, and terminal group differences present in the oligomer side chains will be discussed accordingly.

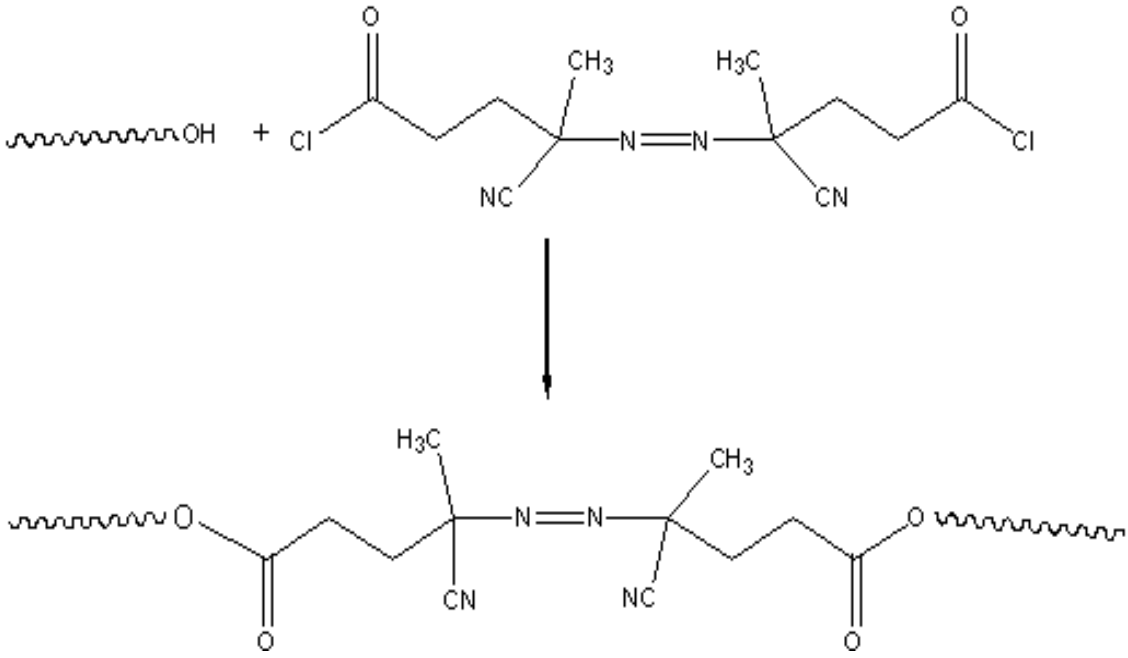

Figure 2.2. Schematic representation of the esterification reaction in the second step

2.2. Experimental

2.2.1. Reagents

Materials. 4,4-Azobis (4-cyanovaleric acid), ($C_6H_8N_4O_4$, MW = 280g/mol, purity > 95%, Wako Chemicals, Japan), 1H, 1H, 11H-Perfluoroundecan-1-ol, ($HCF_2(CF_2)_9CH_2OH$, MW = 532g/mol, purity > 96%, Nalgene HDPE), Perfluorohexyl Ethanol, ($CF_3(CF_2)_5CH_2CH_2OH$, MW = 370g/mol, purity > 97.5%, Glariant GmbH, Frankfurt, Germany).

Solvents and drying agents. Thionyl chloride, ($SOCl_2$, MW = 118.97g/mol, purity > 99%), Hexane (C_6H_{14}, MW = 86g/mol, industrial grade), Tetrahydrofuran, (C_4H_8O, MW = 72.11g/mol, purity > 99%, Sigma-Aldrich, Seelze, Germany), Freon-113 ($C_2Cl_3F_3$, MW = 187.5, purity > 99.9%, BASF, Germany), Pyridine, (C_5H_5N, MW = 79.10g/mol, purity > 99.0%, Lab-Scan, Dublin, Ireland), Calcium Chloride ($CaCl_2$, MW = 110.99g/mol, purity > 95%, J.J. Backer, Deventer, Holland), Sodium Sulfate (anhydrous), (Na_2SO_4, MW = 142.04g/mol, purity > 99.5%, J.J. Backer, Deventer, Holland), Sodium Hydrogen Carbonate, (Na_2HCO_3, MW = 84.01g/mol, purity > 99 – 100.5%, Sigma-Aldrich, Seelze, Germany),

Ethanol, (C_2H_6O, MW = 46.07g/mol, purity > 99.8%),

Chloroform, ($CHCl_3$, MW = 119.38g/mol, purity > 99.9%),

Methanol, (CH_3OH, MW = 32.04g/mol, purity > 99.9%),

all from Labkim, Okmeydani/Istanbul, Turkey.

2.2.2. Characterization

FT-IR spectra were run on Equinox 55/S Fourier transform spectrometer (Brussels, Belgium). Proton NMR, ^{19}F NMR, ^{13}C NMR studies were done in $CDCl_3$ using Unity Inova 500MHz nuclear magnetic resonance (Varian AG, Switzerland). DSC thermal analyses

were run at N_2/N_2 atmosphere in the 0 °C-155 °C temperature range using Netzsch Phoenix diffractional scanning calorimeter 204 (Selb, Germany). STA thermal analyses were run on Netzsch Jupiter simultaneous thermal analysis 449 C (Selb, Germany) equipment.

2.2.3. Isomer Separation of 4,4'-Azobis (4-cyanovaleric acid) (ABCVA)

130g 4,4'-Azobis (4-cyanovaleric acid) was gradually dissolved in ethanol. For this aim, 800mL ethanol was used in three steps till the needed solvent amount for total dissolution was reached. The undissolved acid was collected with centrifugation and labeled as the trans isomer after drying in a vacuum dessicator. 53g of trans isomer was obtained. The remaining solution was subject to vacuum distillation and the cis isomer residue was recovered and dried in a vacuum dessicator. Due to the high sensitivity of the acid, no heating was applied during the distillation process. Instead, cooling of the collector vessel was achieved with liquid nitrogen.

Differential scanning calorimetry (DSC) analysis was carried out for melting point determination. The melting point of the isomer mixture was 131.6 °C. Melting points determined from the thermal analysis of the cis and trans isomers were 122.433 °C and 140.54 °C, respectively. Figures 2.3, 2.4, and 2.5 represent the melting point discrimination utilized by DSC for the isomer mixture, the cis isomer, and the trans isomer, respectively.

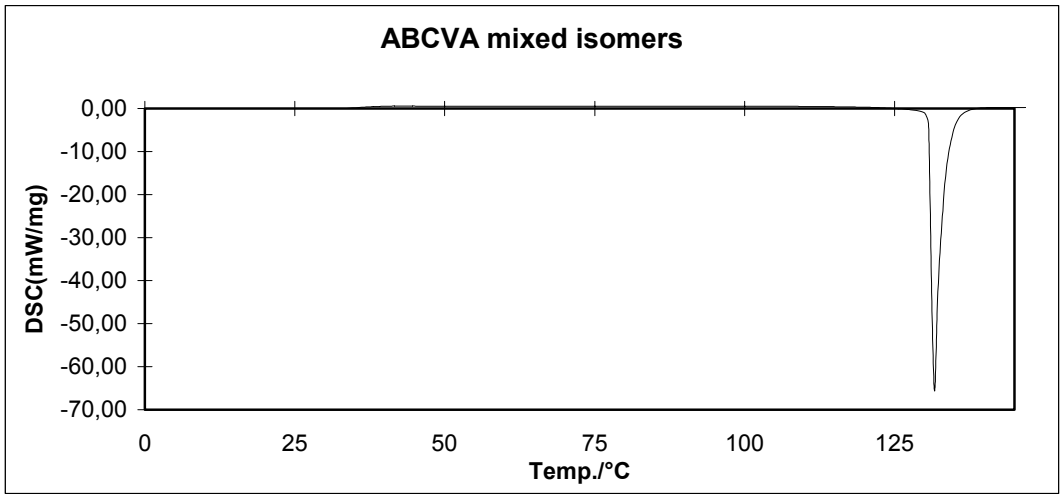

Figure 2.3. DSC of ABCVA isomer mixture

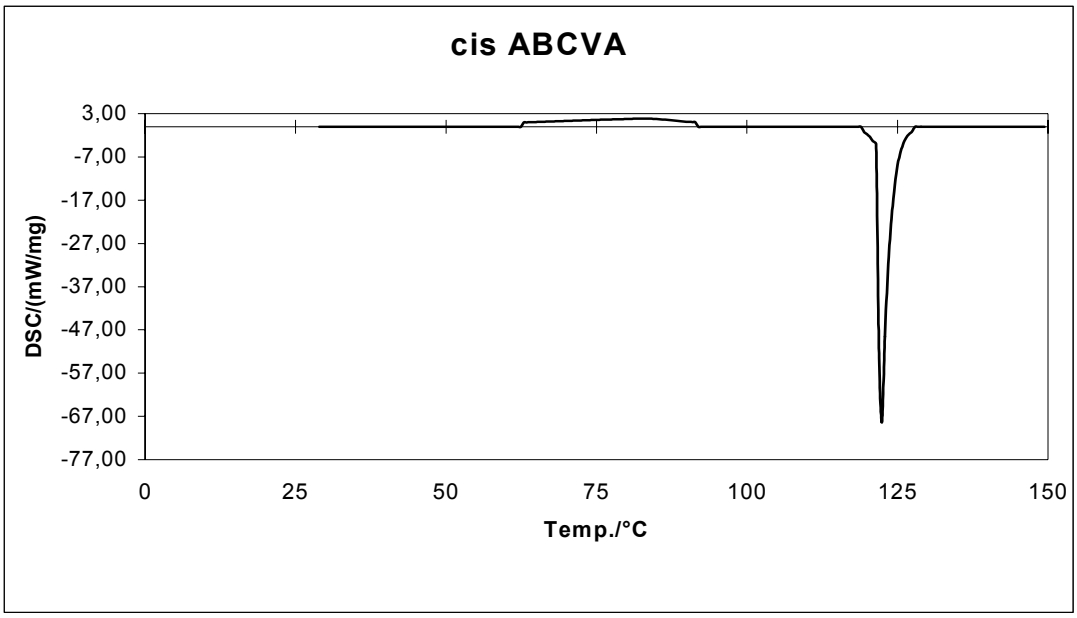

Figure 2.4. DSC of cis isomer ABCVA

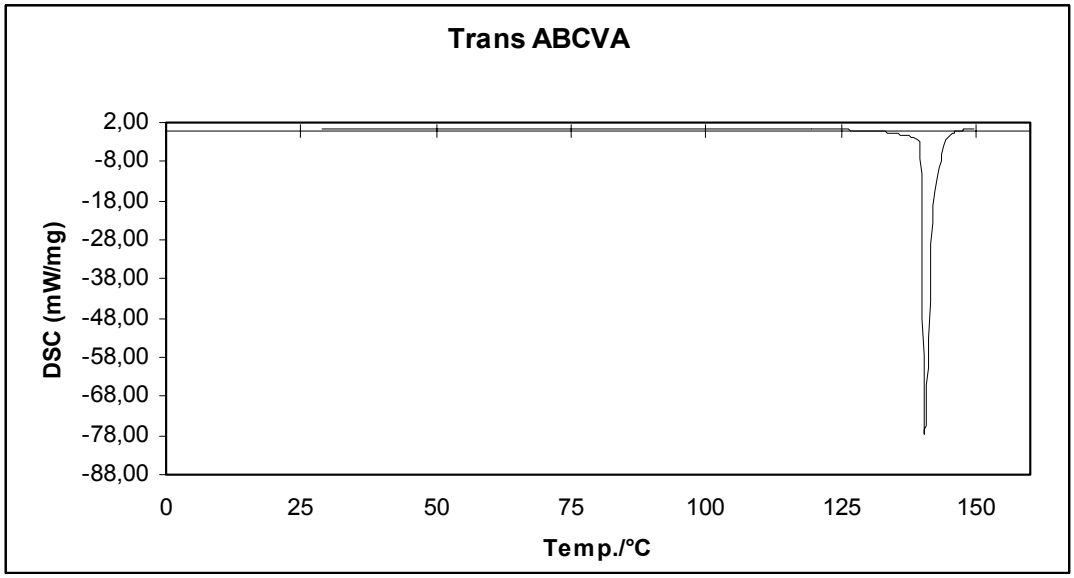

Figure 2.5. DSC of trans isomer of ABCVA

Fourier transform infrared spectra (FT-IR) of the isomers were also obtained and differences in the fingerprint regions were observed. Yet the DSC was used as the main analysis method for separation verification of the isomers. Figure 2.6 represents the spectra of the cis isomer, trans isomer, and the isomer mixture spectra, respectively. The main differences can be observed in the fingerprint regions.

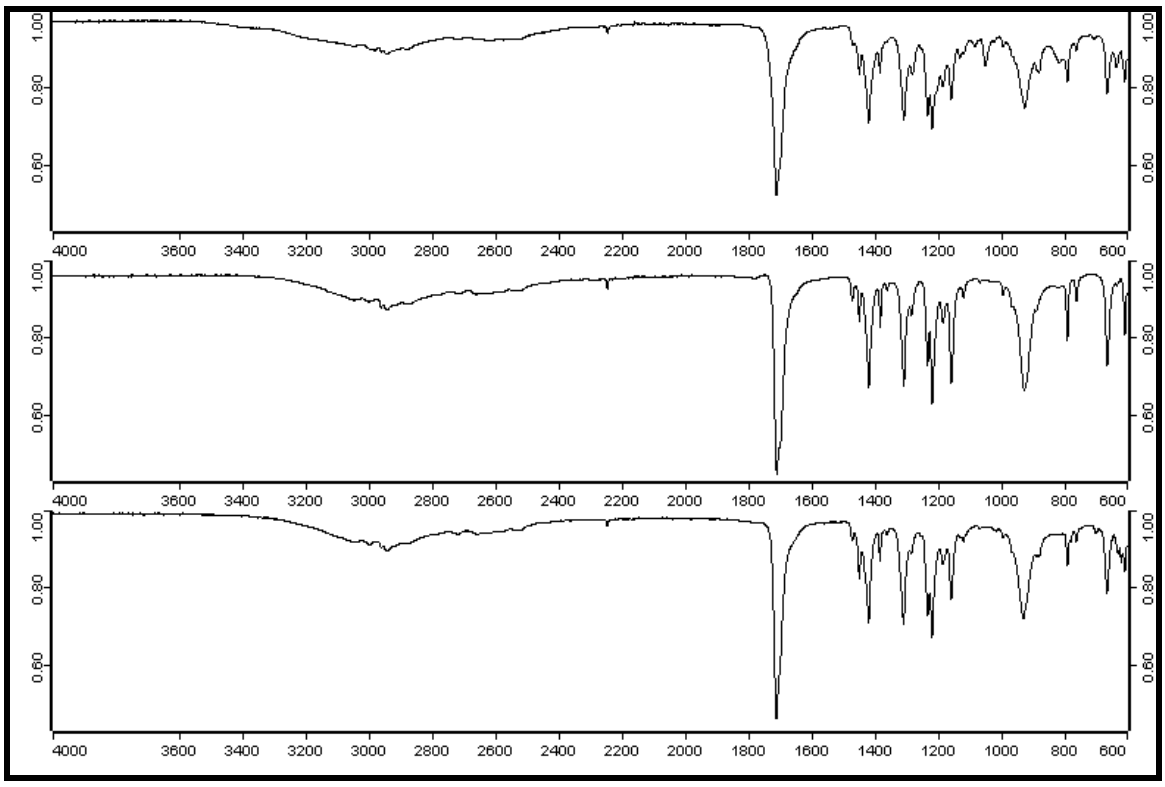

Figure 2.6. Stacked FT-IR spectra of cis ABCVA, trans ABCVA, and isomer mixture, respectively

2.2.4. Synthesis of 4,4'-Azobis (cyanovaleryl chloride) (ABCVCl)

1L hexane was dried over anhydrous sodium sulphate ($NaSO_4$), to be used as a precipitation solvent for the reaction product. The importance of drying is the reason of sensitivity of the product to aqueous media and its easy conversion back to the acid under moisture. 10g trans ABCVA was refluxed with 150ml thionyl chloride ($SOCl_2$) for 50 minutes at 85°C. Then the reaction solution was cooled to room temperature and filtered into 500mL of the previously dried and ice-bath cooled hexane. After filtration, the collected precipitate was washed with the remaining 500mL of cold hexane and dried in a vacuum dessicator over anhydrous calcium chloride, $CaCl_2$.[30] Yield was 95%. Figure 2.7 illustrates the FT-IR spectra of trans ABCVA and trans ABCVCl, stacked respectively. By the same procedure the cis-isomer was reacted too this time for shorter period of 20 minutes and similarly stored under dry conditions. Since the reaction with the trans isomer could be better controlled and the product was obtained at higher conversions, the trans isomer product was mainly used for further reactions. The cis isomer could not be totally converted to ABCVA, since as represented the FT-IR spectra illustrated by Figure 2.8, some non-reacted acid remained at the end of the reaction. Cis ABCVA and cis ABCVCl are stacked respectively. The carbonyl chloride peak was obtained at 1800cm^{-1}. Characteristic CN peak was obtained at 2242 cm^{-1}.[31]

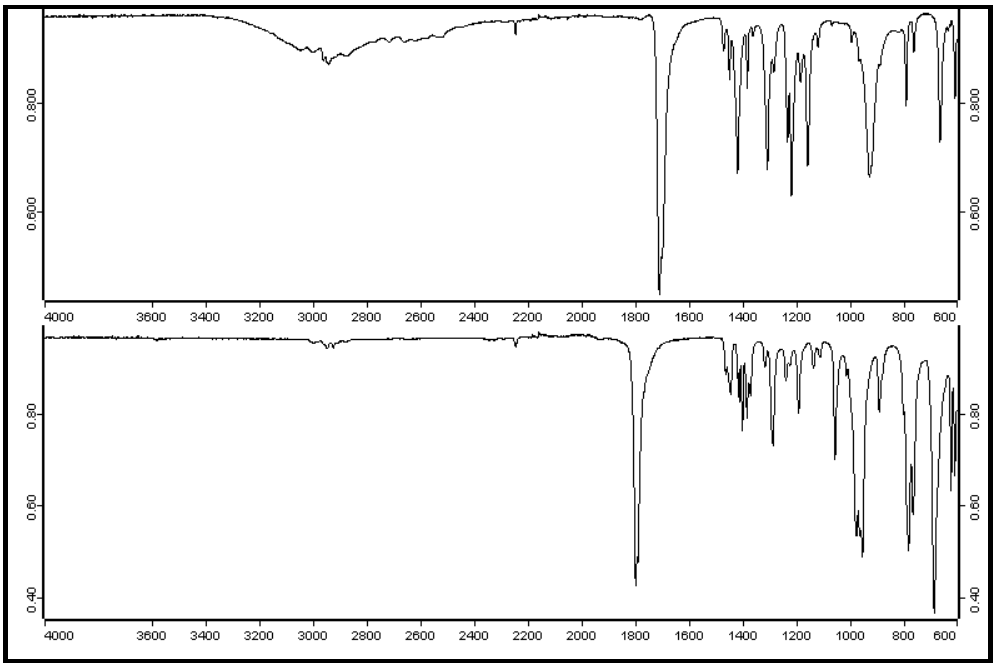

Figure 2.7. Stacked FT-IR spectra of trans ABCVA and trans ABCVCl

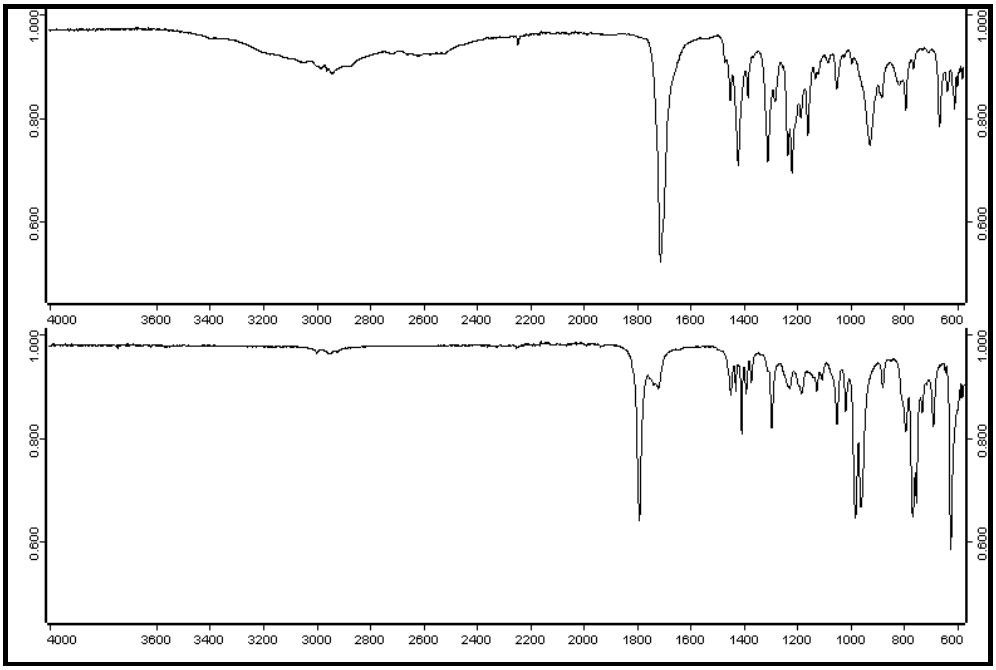

Figure 2.8. FT-IR spectra of cis ABCVA and cis ABCVCl

2.2.5. Synthesis of Fluorinated Azo-Initiators

2.2.5.1. Fluoroinitiator A

19g of the first alcohol labeled as fluoroalcohol A, (1H, 1H, 11H-Perfluoroundecan-1-ol, $HCF_2(CF_2)_9CH_2OH$) was dissolved in 40mL of Freon-113 (1,1,2-trichloro-1,2,2-trifluoroethane). Freon is used to obtain good homogeneity that is helps to provide a more efficient reaction in means of conversion. 1.5mL pyridine was added as phase transfer catalyst. In a separate flask, 5g of ABCVCl was dissolved in 100ml tetrahydrofuran (THF) and slowly added to the first solution. The reaction was carried out under nitrogen atmosphere at room temperature (25 °C) and was let to continue overnight. Then, the pyridine hydrochloride salt that formed was filtered away and the solution was concentrated and dried in a vacuum dessicator as explained previously. The product was washed with aqueous sodium bicarbonate (Na_2HCO_3) solution in order to remove the pyridine hydrochloride salt and any unreacted acid that might be present in ABCVCl left from previous reaction. Yield is 61%.

FT-IR: No alcohol peak at 3350 cm^{-1} corresponding to the hydroxyl (-OH) group of the fluorinated alcohol was observed. Ester peak was observed at 1636 cm^{-1}. Characteristic CN peak is at 2242 cm^{-1}, and CF absorptions are observed at 1136 cm^{-1} and 1192 cm^{-1}, respectively.[31] Figure 2.9 illustrates the stacked FT-IR spectra of trans ABCVCl, product (Fluoroinitiator A) obtained form the esterification reaction of trans ABCVCl and fluoroalcohol A, and the fluoroalcohol A, respectively. A small non-reacted acid peak is observed together with the ester peak. Figure 2.10 is added to make possible the clearer examination of product's spectrum, since the CN peak is very small and difficult to detect in the stacked spectra form.

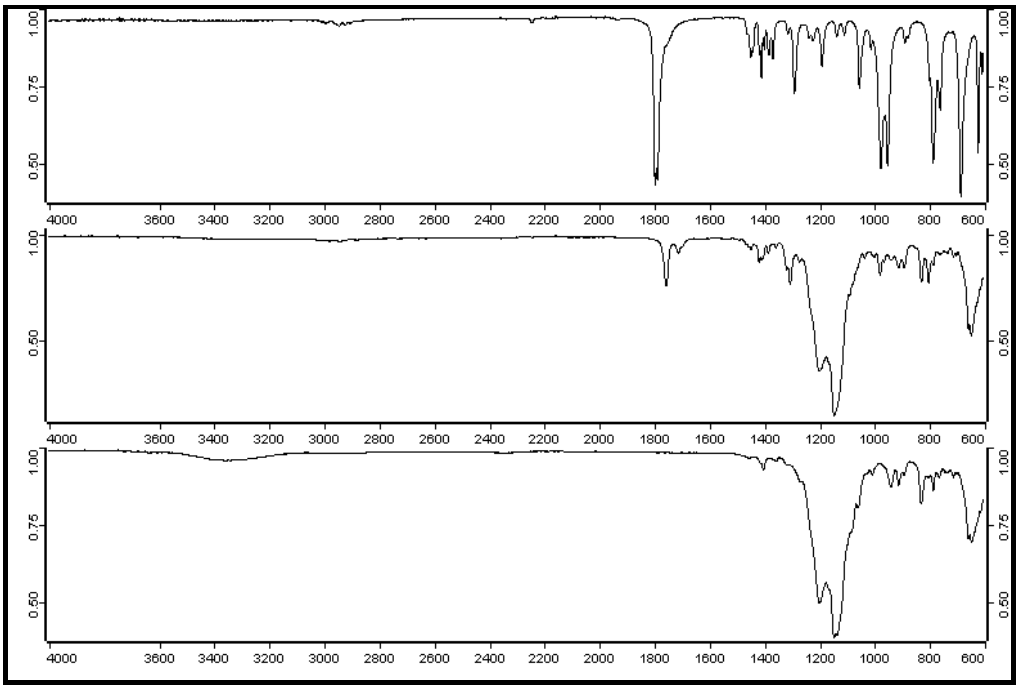

Figure 2.9. FT-IR spectra of trans ABCVA, Fluoroinitiator A, and Fluoroalcohol A, stacked respectively.

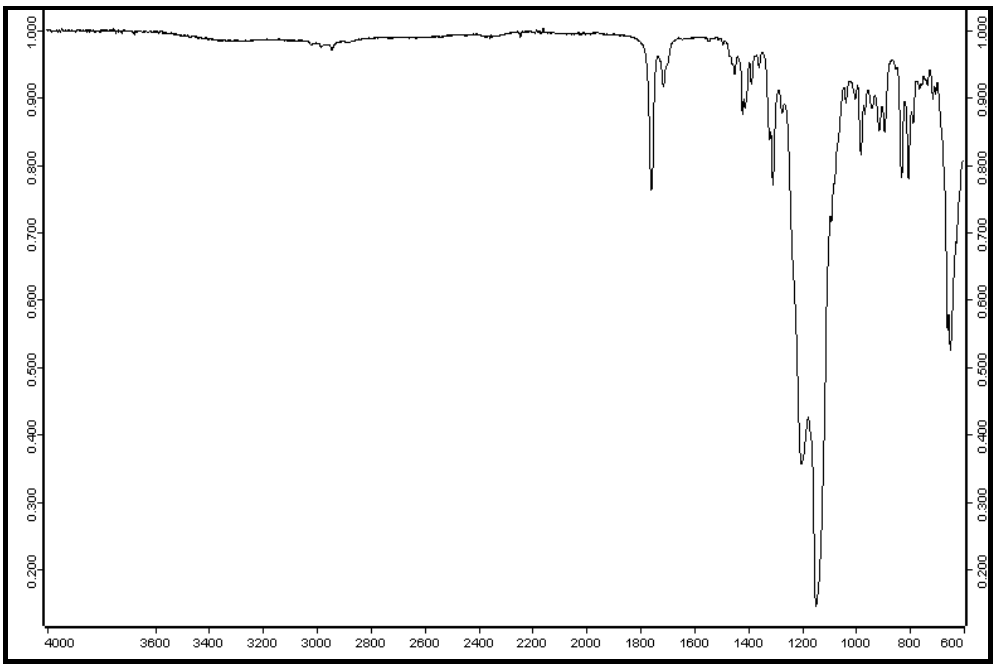

Figure 2.10. FT-IR spectra of Fluoroinitiator A

H^1 NMR: ($CDCl_3$/Freon-113): δ 1.65 (s, 6 H, $-CH_3$), δ 2.4-2.8 (m, 4 H, -OOC-($\underline{CH_2}$)$_2$-C), δ 4-4.2 (t, 4H,-CF_2-CH_2-OOC-), and δ 4.6-4.8 (t, 4 H, -OOC-$\underline{CH_2}$-CH_2-C).[32] Figure 2.11 illustrates the proton NMR spectra of Fluoroinitiator A.

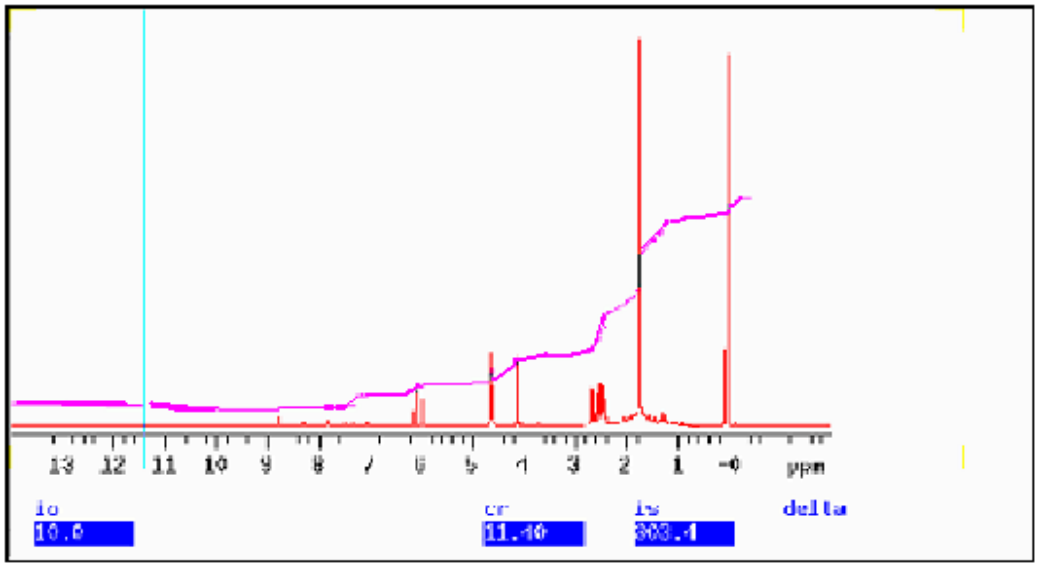

Figure 2.11. Proton NMR spectra of Fluoroinitiator A

Figure 2.12 illustrates the fluorine NMR of Fluoroinitiator A. Figure 2.13 represents the same spectra, this time zoomed into a smaller range where the end group fluorine atoms' duplets can be observed. The signal of these fluorine atoms is split due to coupling caused by the extra hydrogen atom present on the end group. The signal is detected between -139.2 to –139.04 ppm.[33]

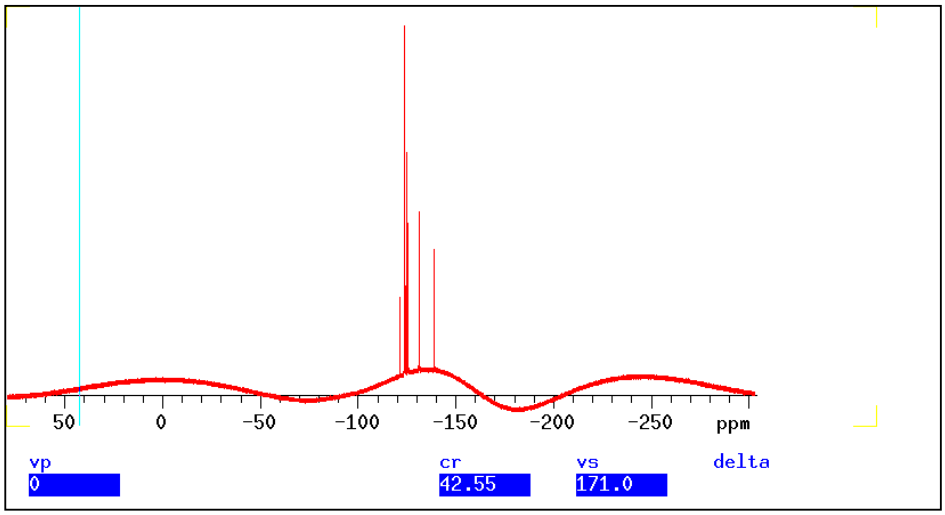

Figure 2.12. ^{19}F NMR spectra of Fluoroinitiator A (wide range)

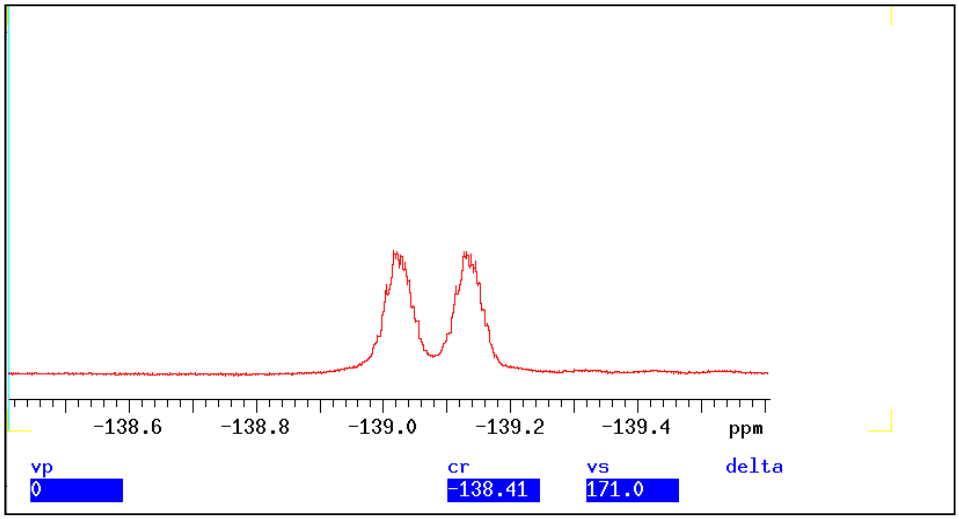

Figure 2.13. ^{19}F NMR spectra of Fluoroinitiator A (narrow range)

2.2.5.2. Fluoroinitiator B

14g of the second alcohol labeled as B perfluorohexyl ethanol, $F(CF_2)_6CH_2CH_2OH$), was reacted with ABCVCl by the same reaction process carried for the synthesis of Fluoroinitiator A. The new initiator contains no hydrogen atoms on the end group of the fluorine segment. Yield is 97%.

FT-IR: Again, no alcohol peak at 3350 cm^{-1} corresponding to the hydroxyl (-OH) group of the fluorinated alcohol was observed. Ester peak was observed at 1636 cm^{-1}. Characteristic CN peak is at 2242 cm-1, and characteristic CF peaks are at the 1100cm^{-1}-1300cm^{-1} region. Figure 2.14 illustrates the stacked FT-IR spectra of trans ABCVCl, product (Fluoroinitiator B) obtained form the esterification reaction of trans ABCVCl and fluoroalcohol B, and the fluoroalcohol B, respectively. Figure 2.15 is again added to make possible the detection of the CN peak, which even in this larger sized spectrum is still difficult to be observed. The higher conversion to product is clearly observed when compared with the spectrum of Fluoroinitiator A. There is no non-reacted acid left.

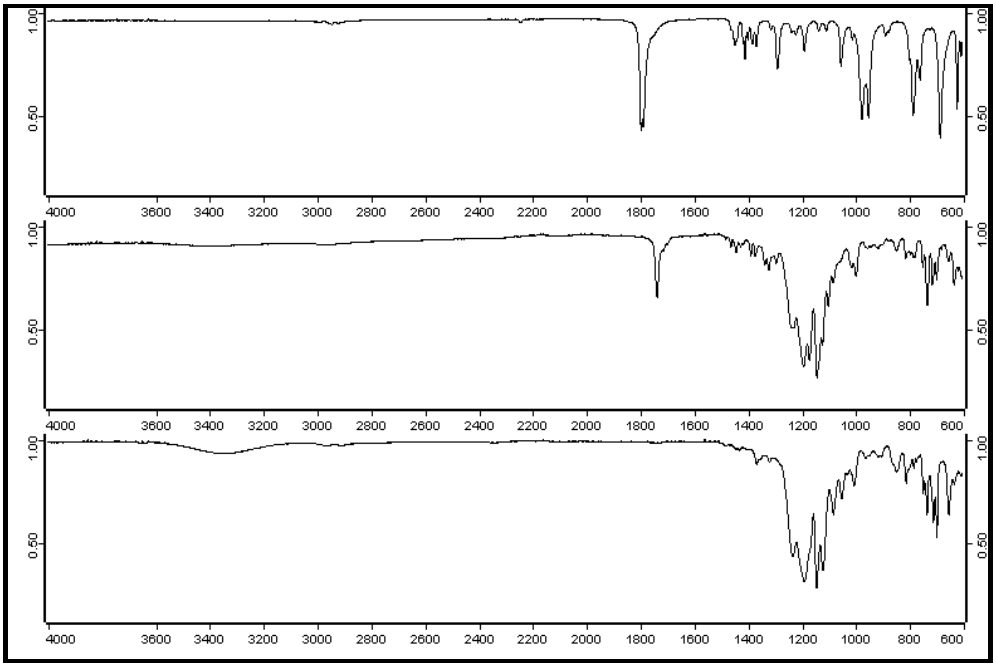

Figure 2.14. FT-IR spectra of trans ABCVA, Fluoroinitiator B, and Fluoroalcohol B, stacked respectively

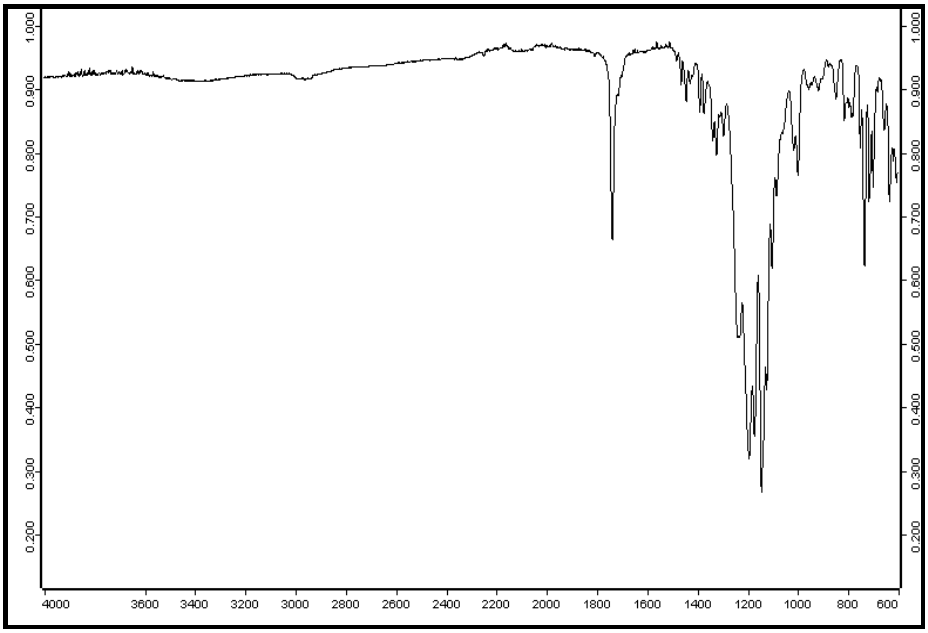

Figure 2.15. FT-IR spectra of Fluoroinitiator B

H^1 NMR: ($CDCl_3$/Freon-113): δ 1.75 (s, 6 H, $-CH_3$), δ 2.3-2.8 (m, 12 H, -OOC-($\underline{CH_2}$)$_2$-C and $-CF_2-\underline{CH_2}-CH_2-OOC-$), δ 4.3-4.8 (t, 4 H, $-CF_2-CH_2-\underline{CH_2}-OOC-$).[32] Figure 2.16 illustrates the proton NMR spectra of Fluoroinitiator B.

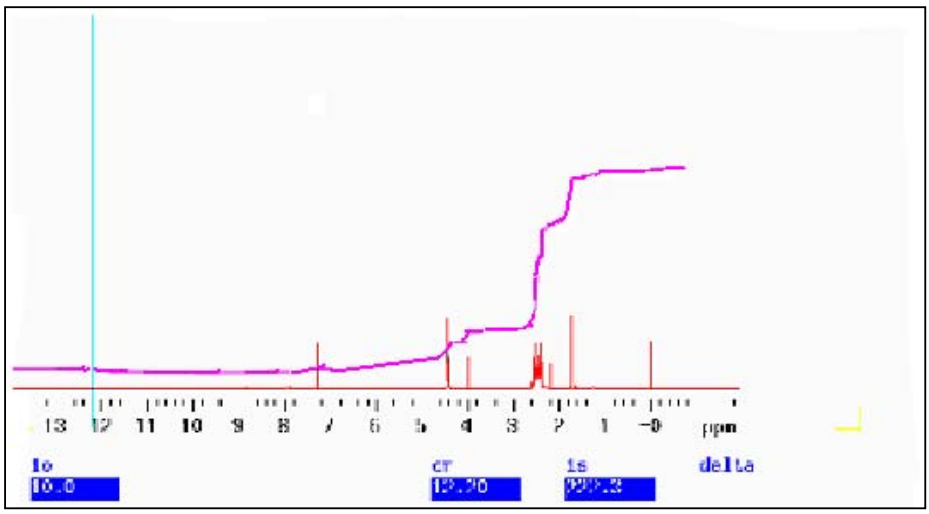

Figure 2.16. Proton NMR spectra of Fluoroinitiator B

Figure 2.17 illustrates the fluorine NMR of Fluoroinitiator B. Figure 2.18 represents the same spectra, this time zoomed into a smaller range where the end group fluorine atoms' triplets can be observed. The end group of this initiator does not have any hydrogen atom(s) and signal of its fluorine atoms is split to three by the fluorines of the neighboring carbon. The signal is detected between –83.0 to – 82.9 ppm.[33]

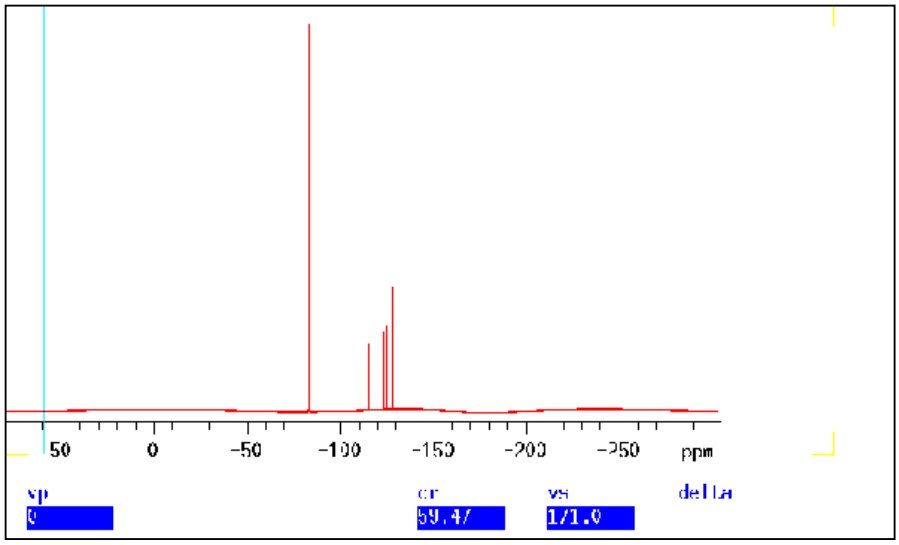

Figure 2.17. [19]F NMR spectra of Fluoroinitiator B (wide range)

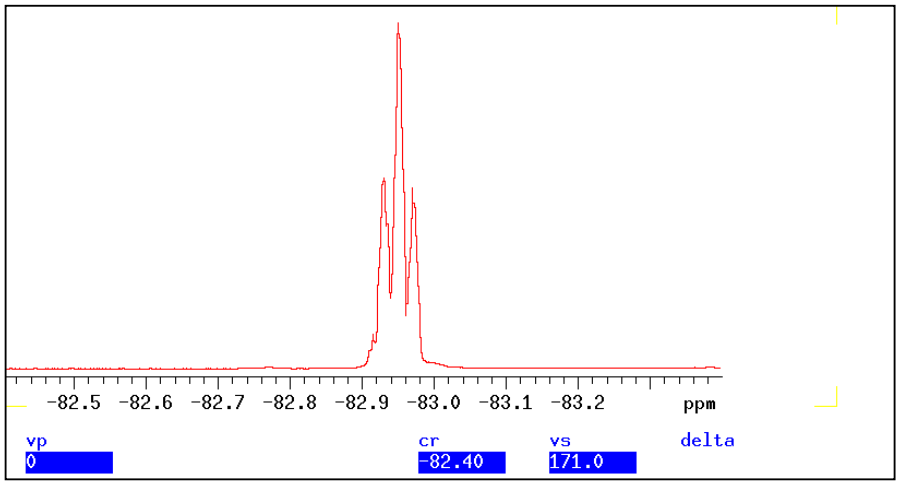

Figure 2.18. [19]F NMR spectra of Fluoroinitiator B (narrow range)

2.2.6. Kinetics of Fluroinitiator B

Many organic molecules are stable even at elevated temperatures (over 400 K). The bonds between the atoms of these molecules are highly stable having strong dissociation energies (BDE) with energies in the 350-500 kJ mol^{-1} ranges. On the other hand, radical initiators have one or more weak bonds with BDE in the 100-200 kJ mol^{-1} ranges. When the temperature is raised high enough, these weak bonds break and the initiator decomposes to produce free radicals.[34]

There are different mechanisms of radical propagation. If a precursor (initiator) is irritated to generate free radicals and if there are available reactive species (generally a double bond), the radicals will react through different mechanisms according to the type of the radical produced. Kinetic studies are beyond the scope of this work. However several kinetic experiments previously conducted by Menceloglu[8] are presented before proceeding to the next chapter. These deal with the synthesis of oligomers through radical polymerization reactions. The aim is to show patterns of initiator decomposition in $scCO_2$ and the temperature dependence of this decomposition process. In the figures below, A is the decomposition rate constant and E_a is the activation energy.

For a unimolecular decomposition mechanism, reaction rate and activation energy dependence on temperature is stated by the Arrhenius equation:[35]

$$A = A_0 \, e^{-Ea/RT} \qquad (2.1)$$

where the pre-exponential factor A_0 is assumed to be independent of temperature. R is the gas constant, and T is the temperature in K.[35] The natural logarithm of the equation leads to:

$$\ln (A_0/A) = E_a /RT \qquad (2.2)$$

From the plot of ln A versus $1/T$ the activation energy (E_a) can be obtained. There is a linear dependence between ln A and $1/T$. Decomposition patterns are observed in $scCO_2$. Arrhenius plots are also obtained from DSC thermal analysis and UV-spectroscopic

analysis. Activation energies are obtained from the slope of the plots. Figure 2.19 illustrates the plot of ln (A_0/A) vs. time, for Fluoroinitiator B decomposition in CO_2 at 3000 PSI. The k_d values at 60 °C, 70 °C, and 80 °C are 7.8 x 10^{-6} sec^{-1}, 15.6 x 10^{-6} sec^{-1}, and 36.4 x 10^{-6} sec^{-1}, respectively.

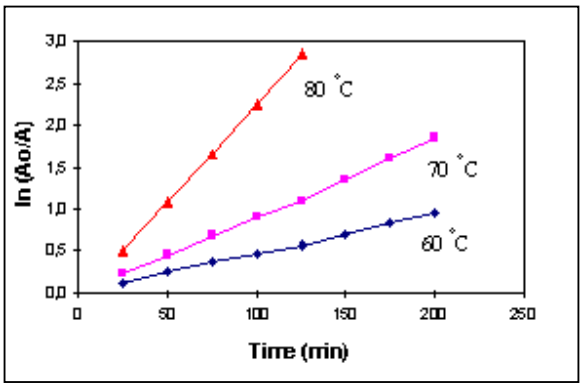

Figure 2.19. Plot of ln (A_0/A) vs. time, for Fluoroinitiator decomposition in CO_2.

Figure 2.20 illustrates the Arrhenius plot of Fluoroinitiator B obtained by UV (Ultraviolet Spectroscopy). The experiment is conducted in $scCO_2$. The activation energy obtained is E_a = 75 .7 kJ/mol.

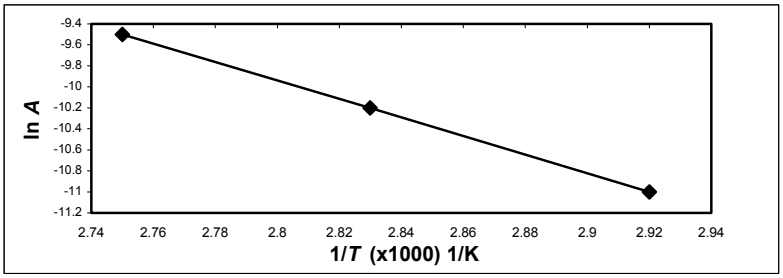

Figure 2.20. Arrhenius plot of Fluoroinitiator B by UV

Figure 2.21 illustrates the Arrhenius plot of Fluoroinitiator B obtained by DSC. The experiment is conducted in 2-chlorobenzyl trifluoride. The activation energy obtained is E_a = 181.1 kJ/mol.

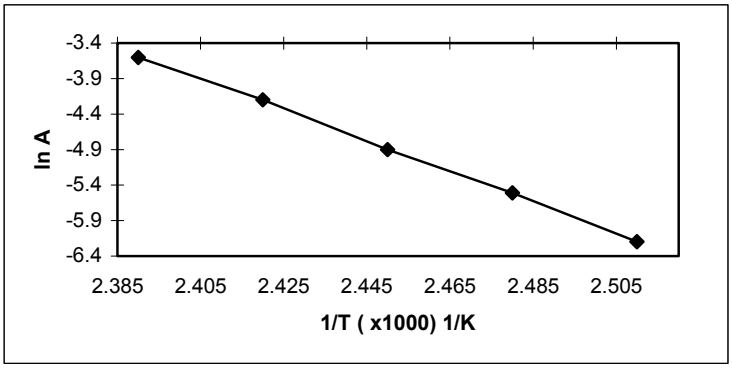

Figure 2.21. Arrhenius plot of Fluoroinitiator B by DSC

.

2.3. Results and Discussion

2.3.1. Isomer separation of 4,4'-Azobis (4-cyanovaleric acid) (ABCVA)

The cis and trans mixture of ABCVA gives a melting point that is in between the melting points of the two isomers. This is an expected observation, since the two isomers have different melting points. In the mixed form, isomers are approximately in the same content as determined after the separation.

After comparing the results obtained by different characterization methods such as FT-IR, NMR and DSC, it is concluded that the melting point determination is the best method to verify the separation, since melting point difference is one of the most discriminative properties of isomers.

2.3.2. Synthesis of 4,4'-Azobis (cyanovaleryl chloride) (ABCVCl)

The FT-IR characterization was the main method to verify the reaction completion and the conversion degree to the product. The main difference in the spectra of ABCVA and ABCVCl is the different vibration frequencies of the their carbonyl groups. The former

one has an acidic carbonyl and the vibration frequency is expected to be lower than the latter's acyl chloride vibration frequency. This is verified in the result. Also the conversion degree can be clearly followed. In case that any unreacted acid remains, the acidic carbonyl peak will be present in the spectrum too.

Another important issue that is to be considered is the fact that overreacting the acid causes decomposition. This is again followed in the spectrum as a shift in the vibration frequency of the carbonyl group. By running the reaction several times to estimate an optimum reaction time, the exact needed time for total conversion is found. This period is different for the two acid isomers as mentioned before. For both isomers, optimum reaction times were estimated and total conversion to product was achieved successfully.

2.3.3. Synthesis of Fluorinated Azo-Initiators

Both of the Fluoroinitiators A and B were synthesized under the same conditions. The main difference is in the fluorine segment. The first one has a higher fluorine atom content and additional hydrogen atom at the end of the chain. During the synthesis the main problem that was encountered was the separation of unreacted species from the product. The second product, Fluoroinitiator B, was obtained in the pure form much easily and washing the product was just carried out to ensure the absence of any impurity. However, the first product required much more washing to get the highest maximum purity. Thus the second initiator was obtained in higher yield than the first one, since it was mainly lost during the washing procedures.

The FT-IR spectra of the products verified the conversion to product with an ester peak at the characteristic frequency range. Other expected peaks of the CF and CN groups were also present at the characteristic vibration frequency ranges.

Proton NMR, ^{19}F NMR, ^{13}C NMR studies were very much helpful in the characterization studies of the products. Fluoroinitiator A's spectra showed small amount of unreacted alcohol. The end group differentiation was mainly achieved by ^{19}F NMR studies.

The final conclusion is that a hydrogen atom present at one end (the opposite end to the one attached to the hydroxyl group) of the alcohol causes completion in the reaction.

During the reaction, it is involved in undesired intermolecular interactions that decrease the efficiency of the reaction. The hydrogen atom is capable of making hydrogen bonding with electronegative elements such as nitrogen, oxygen, and fluorine.[36] Any hydrogen bonding caused by the hydrogen present on the end group can causes complications ending in a more sterically hindered structure, which in turn decreases the availability of the hydroxylic hydrogen to the reactive sides. The result is a lower yield and lower conversion to product. The intermolecular interactions caused by the extra hydrogen atom can also be verified by the difficulty encountered during efforts made to dissolve Fluoroinitiator A in several polar and fluorinated solvents that are normally expected to dissolve the product. The same problem is not encountered with Fluoroinitiator B, which is easily dissolved in highly polar solvents such as THF, chloroform, etc.

CHAPTER 3

SYNTHESIS OF FLUORINATED BLOCK OLIGOMERS

3.1. Introduction

This chapter describes of the synthesis of fluorinated segments containing block oligomers that are designed for supercritical CO_2 applications. For this aim, several available monomers are selected and polymerization reactions are run under the same conditions for each reaction set using the previously synthesized fluorinated azo initiators (Fluoroinitiators A and B).

Two sets of oligomers are synthesized: One with Fluoroinitiator A, and the second one with Fluoroinitiator B. The sets are labeled as Set 1 and Set 2, respectively. The main differences between the two set's oligomers are the end group character of their fluorine segments (Set 1 group contains a hydrogen atom in the end group of the fluorine segments while Set 2 fluorine segments' end groups consist only of carbon and fluorine atoms) and the number of CH_2 spacer groups to the ester group (Set 1 oligomers contain one CH_2 spacer group, while Set 2 oligomers contain two CH_2 spacer groups). Basic analyses such as TG, DSC and FT-IR are carried out in order to characterize the products. In this way, information about decomposition patterns, stabilities, glass transition point (Tg), and functional groups is obtained. In addition GPC and NMR analyses are carried out for molecular weight determination. The oligomers' solubility in $scCO_2$ is tested and the effect of the end group character is investigated. Predictions for dissolution patterns are made

with the help of previously conducted molecular dynamic simulation experiments by Kirmizialtin et al. According to these calculations the surfactant systems form bilayered micelles, with CO_2-phobic segments stuck in the middle and fluorine segment preserved in their normal vacuum conformation.[11] Thus, in a simple system containing two immiscible phases (one being sc CO_2) and a surfactant component, the fluorinated groups of the surfactant act as the CO_2 compatible, more free segments that interact with the supercritical fluid phase, and the inner part of the micelle, the hydrocarbon part interacts with the CO_2-phobic phase.

Another result of Kirmizialtin's work was the investigation of molecular interactions that dominated in solubility patterns of the oligomers. It was shown that the dominant effect was that of the van der Waals interactions when compared to the effect of the electrostatic interactions. Here, van der Waals forces describe the dispersion forces. The origin of these forces is temporary fluctuating dipoles. They are strongly affected by the size of molecules and atoms. As the size increases, the space available for electron movement increases too and the interaction gets stronger. These forces are also affected by molecular shape. Longer and thinner molecules can align more easily and provide better interaction compared to short and branched ones.[36] This is the basic explanation of the steric effect. The more steric a molecule is, the less it is available for interacting species.

The selection of monomers is accomplished accordingly with previously performed computational experiments for the prediction of sc CO_2 solubility of different oligomers.[11] The selected monomers are vinylic type compounds that when reacted by a radical polymerization mechanism result in co-oligomers with repeating units having the general formula of -(-CH_2-CRH-)-.

3.2. Experimental

3.2.1. Reagents

Monomers and initiator. Methyl Methacrylate, MMA ($C_5H_8O_2$, MW = 100g/mol, industrial grade), Styrene (C_8H_8, MW = 104g/mol, industrial grade), Methacryl Amide, MA (C_4H_7NO, MW = 85g/mol, industrial grade), Acrilonitrile, (C_3H_3N, MW = 53g/mol, > 99.5%, Sigma-Aldrich, Seelze, Germany),

Diacetone Acrylamide, DAM ($C_9H_{15}NO_2$, MW = 169.23g/mol, purity > 98%),

4-Hydroxybutyl Acrylate, 4-HBA ($C_7H_{12}O_3$, MW = 144.17g/mol, purity > 95%),

1,4-Cyclohexanedimethanol Monoacrylate, 1,4-CHDMMA ($C_{11}H_{18}O_3$, MW = 198.26g/mol, purity > 95%),

all from Nippon Kasei Chemical Co., LTD, Tokyo, Japan.

Solvents and Drying Agents. Freon ($C_2Cl_3F_3$, MW = 187.5, purity > 99.9%, BASF Germany), Tetrahydrofuran, (C_4H_8O, MW = 72.11g/mol, purity > 99%, Sigma-Aldrich, Seelze, Germany),

Ethanol, (C_2H_6O, MW = 46.07g/mol, purity > 99.8%),

Chloroform, ($CHCl_3$, MW = 119.38g/mol, purity > 99.9%),

Methanol, (CH_3OH, MW = 32.04g/mol, purity > 99.9%),

all from Labkim, Okmeydani/Istanbul, Turkey.

Figure 3.1 illustrates the monomers used for the oligomer syntheses.

3.2.2. Synthesis of Series I

The monomers represented were reacted with Fluoroinitiator A at 85 °C overnight under nitrogen atmosphere. The monomer initiator ratio used was 12/1 by weight. High initiator amount is used in order to guarantee tri-block formation.[37] The solvent used for all syntheses was THF. It was chosen after several trials with various solvents that were conducted in order to find the most efficient solvent for all materials, and was used for all

individual syntheses to set all conditions to be identical for all reactions. Obtained oligomers were purified by precipitation either in ethanol or in water, or in the mixtures of both, according to which one worked the best. All products were dried in vacuum oven at room temperature and a vacuumed dessicator, respectively. Then they were finely grinded and kept in the vacuumed dessicator for characterization analyses. Yields were in the range of 70%-80% due to conversions of intermediate efficiency and some material loss during purification procedures. Figure 3.1 illustrates the monomers used for the oligomer syntheses.

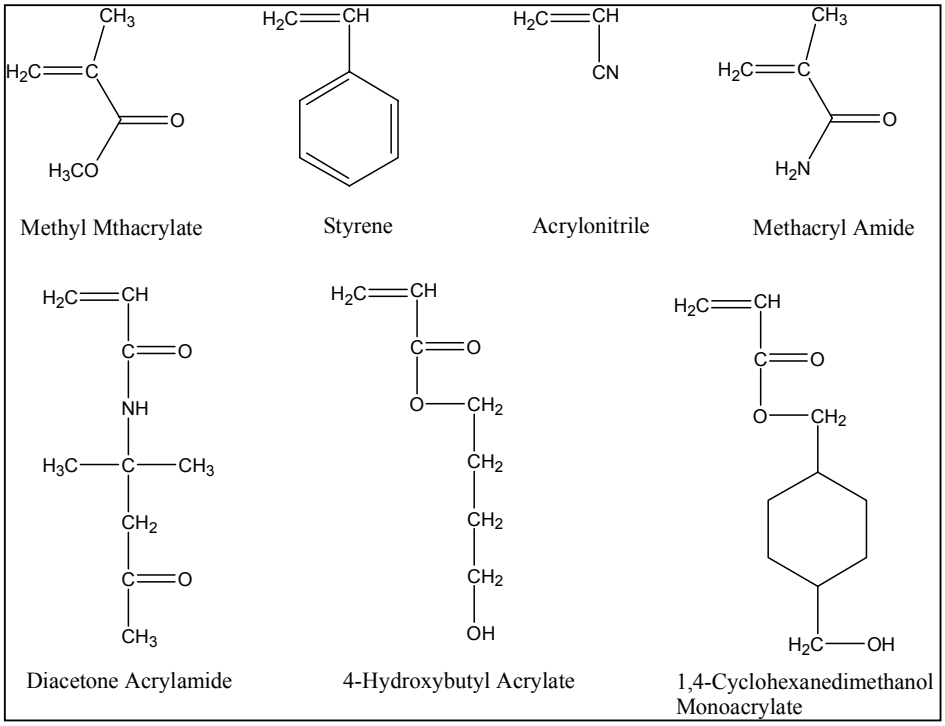

Figure 3.1. Monomers used in the syntheses

Table 3.1 displays the abbreviations used for the oligomers together with the names of the monomers they are synthesized from, on the next page.

Table 3.1. Synthesized Oligomers and the monomers used for their syntheses

Monomers	**Oligomers**
Methyl methacrylate	PMMA
Styrene	PS
Acrylonitrile	PAN
Methyl acrylamide	PAM
4-Hydroxybutyl acrylate	PHBA
Diacetone acrylamide	PDAM
1,4-Cyclohexanedimethanol monoacrylate	PC

3.2.3. Synthesis of Series II

With the same monomers and Fluoroinitiator B, new set of oligomers was synthesized in tubes. Again reaction temperature was set to 85 °C. The reactions were run overnight under nitrogen atmosphere. Monomer/initiator ratio was again kept 12/1. Purification and drying procedures performed for the previous series' syntheses were followed identically. Yields were in the 87%-95% range.

3.2.4. Solubility in $ScCO_2$

The solubility experiments were performed with P-50 High Pressure Pump Contrivance (Pittsburgh, PA, USA). The phase behavior studies were managed using a 50mL high-pressure view cell. The pressure was set to 4000 PSI for all solubility experiments. Initially no heat was applied. Then heat of 40°C was applied by a previously prepared water bath to detect any increase in dissolving efficiency of the solvent on heating. Figure 3.2 illustrates a detailed scheme of the supercritical contrivance utilized in the experiment. Phase behavior of 1mg material in 50mL supercritical fluid was observed. All of the experiments were run for 1h, an optimum period assigned to detect maximum obtainable solubility.

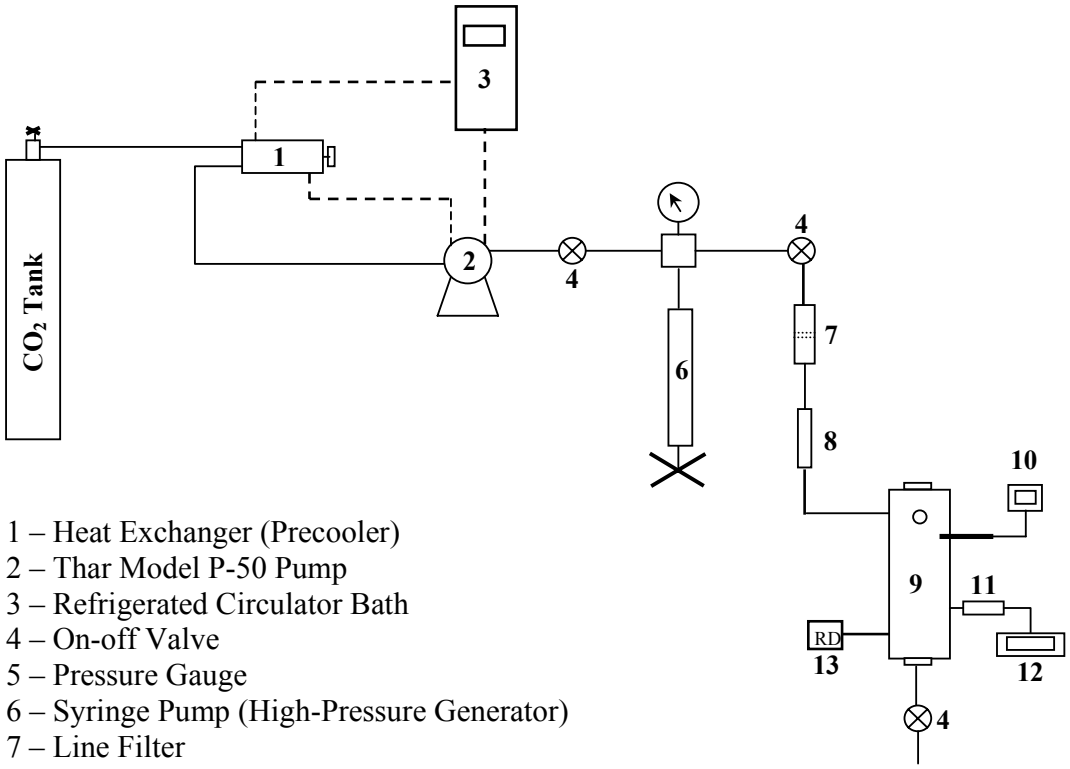

1 – Heat Exchanger (Precooler)
2 – Thar Model P-50 Pump
3 – Refrigerated Circulator Bath
4 – On-off Valve
5 – Pressure Gauge
6 – Syringe Pump (High-Pressure Generator)
7 – Line Filter
8 – Check Valve
9 – Reactor/View cell
10 – Thermocouple and Temperature Read-out
11 – Pressure Transducer
12 – Pressure Read-out
13 – Rupture Disk

Figure 3.2. Schematic representation of the supercritical contrivance

3.2.4.1. Solubility of Series I

The following solubility patterns of the Series I oligomers are obtained and the results are presented in Table 3.2 Most soluble oligomers are PAM-1 and PDAM-1, which are completely miscible with the supercritical phase. After come PHBA-1 and PC-1 with

relatively high solubility efficiencies. PMMA-1 and PAN-1 follow with moderate solubility efficiencies. PS-1 is not soluble. The materials show gradual dissolution patterns. At first, plasticization is observed. Then the material becomes sticky and finally dissolves completely, which is observed as a single phase consisting of dissolved material and supercritical fluid. Some materials do not dissolve completely and small residues are observed as an immiscible phase. These are assigned as highly soluble materials. Table 3.2 describes the dissolution patterns of the materials. The order of materials in the table is from the most soluble to the least soluble.

Table 3.2 Solubility of Series I: oligomers synthesized with Fluoroinitiator A

Oligomer	Solubility	Comments
PAM-1	Readily soluble	Dissolves on initial treatment.
PDAM-1	Readily soluble	Became sticky, continuous dissolution pattern with time.
PC-1	High solubility	Became transparent on treatment.
PHBA-1	High solubility	Plasticized, became sticky transparent.
PAN-1	Moderate soluble	Became sticky and transparent.
PMMA-1	Moderate soluble	Plasticized, became sticky transparent.
PS-1	Not soluble	

3.4.2.2. Solubility of Series II

The solubility experiments with Series II are conducted utilizing the exact experimental conditions and instrumentation of the solubility experiments carried out for Series I. Considerable improvement in the solubility efficiency for the Series II oligomers is observed. PAM-2, PDAM-2, and PC-2 are totally soluble and show complete phase mixing. PMMA-2, PAN-2, and PPHBA-2 are highly soluble. Solubility efficiency of PS-2

improves slightly and low degree of plasticization is observed on treatment. Table 3.3 displays the solubility patterns for Series II oligomers. Again the order of materials in the table is from the most soluble to the least soluble, downwards.

Table 3.3. Solubility of Series II: oligomers synthesized with Fluoroinitiator B

Oligomer	Solubility	Comments
PAM-2	Readily soluble	Dissolves on initial treatment
PDAM-2	Readily soluble	Plasticized, became sticky and finally dissolved completely
PC-2	Readily soluble	First plasticized, became sticky, and finally dissolved totally.
PHBA-2	High solubility	Plasticized, became sticky and transparent
PAN-2	High solubility	Became sticky and transparent
PMMA-2	High solubility	Plasticized, became sticky and transparent
PS-2	Low solubility	Low degree of plasticization observed

3.2.5. Characterization

FT-IR spectra were run on Equinox 55/S Fourier transform spectrometer (Brussels, Belgium). Proton NMR studies were done in $CDCl_3$ using Unity Inova 500MHz nuclear magnetic resonance (Varian AG, Switzerland). DSC thermal analyses were run at N_2/N_2 atmosphere in the 0 °C-155 °C temperature range using Netzsch Phoenix diffractional scanning calorimeter 204 (Selb, Germany). STA thermal analyses were run on Netzsch Jupiter simultaneous thermal analysis 449 C (Selb, Germany) equipment.

3.2.5.1. FT-IR

3.2.5.1.1. Series I

FT-IR of monomer, initiator and oligomer were obtained, respectively. All of the spectra were matched and compared. Characteristic peaks of each monomer and the characteristic peaks of the fluorinated initiator were all present in the oligomer. This was the expected result. As an example, spectrum of PAN-1 is represented Figure 3.4. The order of compounds in the stacked spectra representation is downwards: Fluoroinitiator B, oligomer (PAN-1), and monomer (acrylonitrile), respectively. The expected peaks of functional groups coming from the reactants and that are accordingly present in spectra of the oligomers are: CN peak is at 2242cm^{-1}, and CF absorptions are observed at 1136cm^{-1} and 1192cm^{-1} respectively.

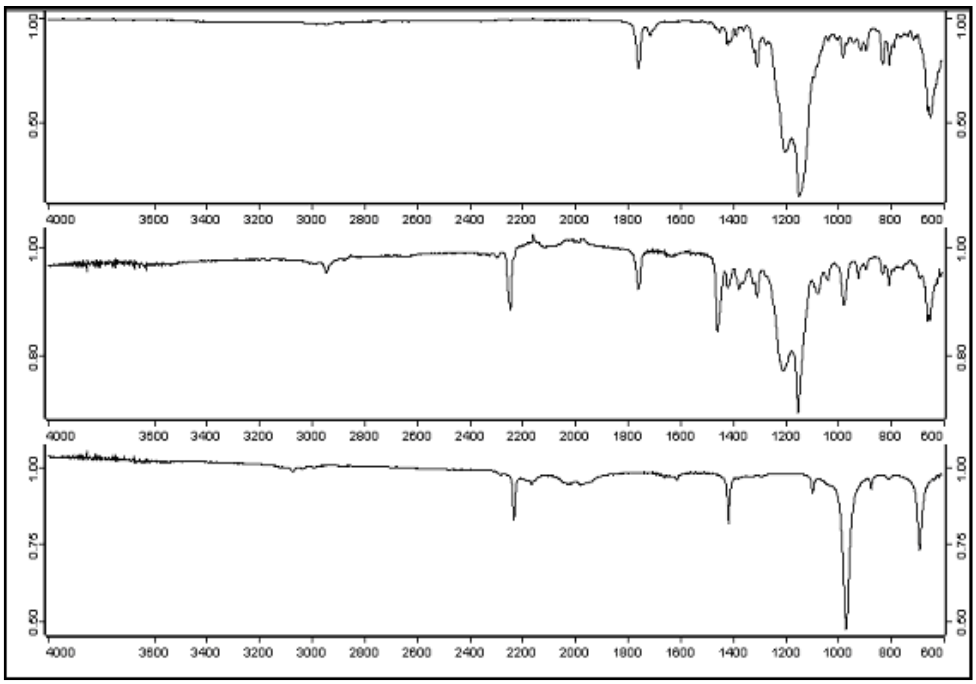

Figure 3.3. FT-IR spectra of Fluoronitiator A, PAN-1, and monomer: acrylonitrile, stacked respectively.

3.2.5.1.2. Series II

Again, FT-IR of monomer, initiator and oligomer were obtained, respectively. The spectra were matched and compared. In order to make a basic comparison with PAN-1 of Series-I, the spectrum of the oligomer synthesized with the same monomer (acrylonitrile) is presented in Figure 3.5. The characteristic peaks of the monomer are again observed together with the characteristic peaks of the initiator: characteristic CN peak is at 2242cm^{-1}, and CF absorptions that are also present in the initiator spectrum are observed at 1300cm^{-1}-1500cm^{-1} frequency range.[31] The main difference between Series I and Series II is defined by the CF peaks of the Fluoronitiators A and B in the 1200-1500cm^{-1} regions. The same trend applies for all of the synthesized oligomers.

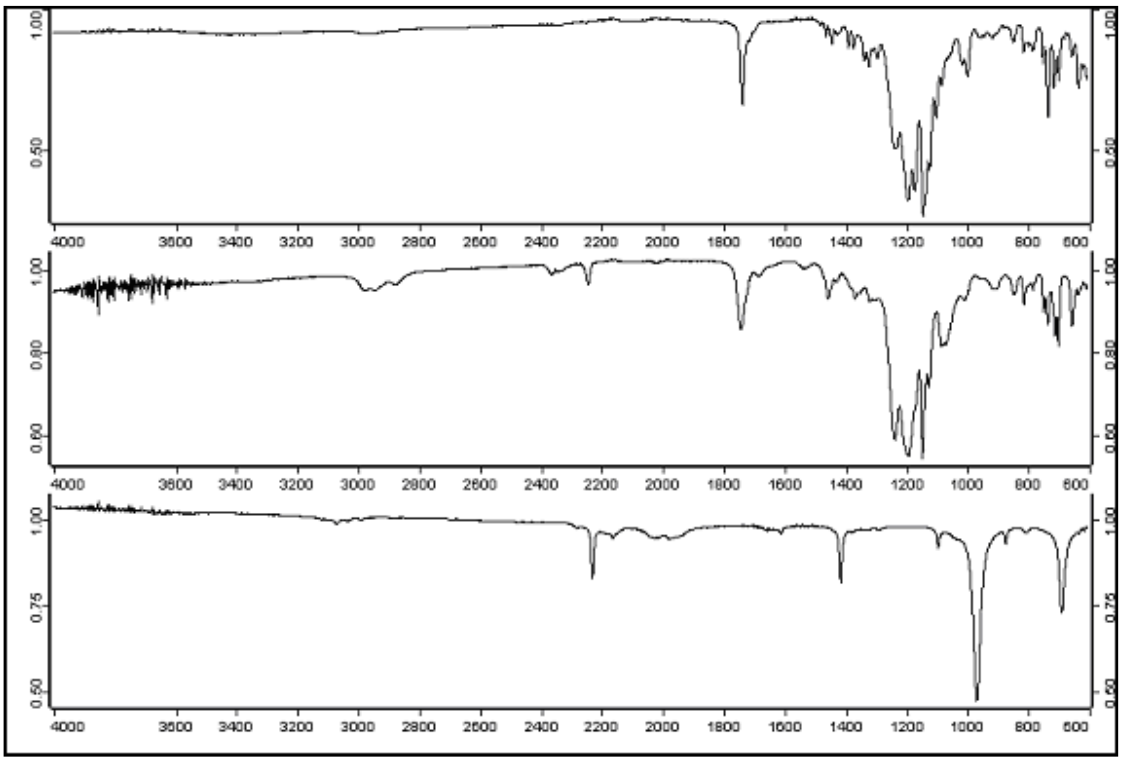

Figure 3.4. FT-IR spectra of Fluoroinitiator B, PAN-2, and monomer: acrylonitrile, stacked respectively

3.2.5.2. Thermogravimetric and Differential Thermal Analyses

Thermal analysis constitutes of methods by which properties of materials are measured as a function of temperature. During the measurements, the materials are subjected to a controlled temperature program. Thermogravimetry (TGA) is generally run together with Differential Thermal Analysis (DTA), and studies mass changes on heating.

Differential Thermal Analysis (DTA) is an efficient device to characterize transformation energies (exothermal energies and endothermal energies).[38] The method consists of heating and cooling the experiment sample and an inert reference. The conditions applied to both are identical and the device records any temperature difference between the sample and the reference. Then the plot of this differential temperature versus time or temperature is obtained. In this way, the changes in the sample are detected by analyzing the heat absorption and evolution patterns.[39] Actually Differential Scanning Calorimetry is a very satisfying method alone to study Tg (glass-transition temperature), crystallinity patterns, stability and purity of polymeric materials alone (explained in much detail in the next section). DTA gives information about the thermal stability, polymer content and similar information that can also be obtained by DSC. TGA itself is what gives the main additional information about the decomposition patterns of the polymer by detecting mass change on heating.[40] In this work, the main concern is to obtain basic information about crystallinity, Tg points and phase transitions such as melting, and finally make relation with materials' solubilities in $scCO_2$. The DSC instrument itself is quite efficient for this aim, but due to its high sensitivity to contaminations at elevated temperatures, the first oligomer series are also analyzed with the TGA instrument in order to detect the common decomposition patterns of materials and set an appropriate, optimum temperature range for the DSC analyses. After all, few TGA analyses are present in the paper as representative examples.

The thermal decomposition trends of the oligomers were investigated with differential thermal and thermo gravimetric analyses (DTA and TG). Temperature range was set from 35^0C to 600^0C under nitrogen atmosphere. Heating rate was set to 10 °C/min.

3.2.5.2.1. Series I

The analysis showed that all oligomers except PS-1 have initial decomposition in the range of 135 °C - 275 °C temperatures. PS-1 has relatively high initial decomposition temperature around 395 °C. This shows that PS-1 is relatively more stable than all and this behavior can be attributed to high molecular weight.[40] PMMA-1 and PAM-1 have similar decomposition patterns with initial mass changes in the 150 °C - 250 °C temperature range (consistent result with their chemical structure similarities). PAN-1 and PC-1 have initial mass changes in the 135 °C - 150 °C temperature range, and similarly PHBA-1 and PDAM-1 have initial mass changes in the 95 °C - 135 °C range. Figure 3.5 and Figure 3.6 are representative illustrations of the decomposition behaviors of PS-1 and PMMA-1, respectively. The two figures represent two types of decomposition patterns observed for the oligomers on the whole. PS-1 shows a very large mass loss that can be attributed to high quantity gas evolvement.[41] The loss of volatile material in PMMA-1 is much lower. Gradual stepwise decomposition is observed.

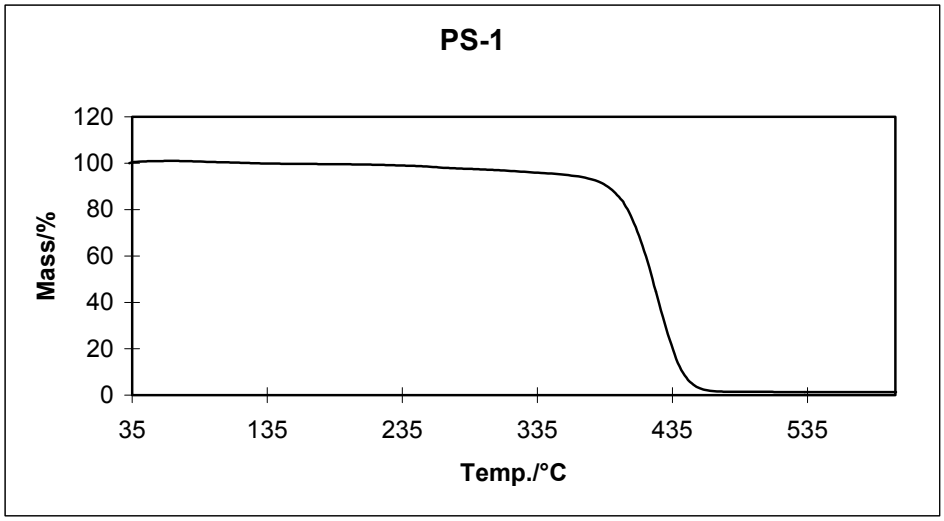

Figure 3.5. TG analysis of polystyrene-1 (PS-1)

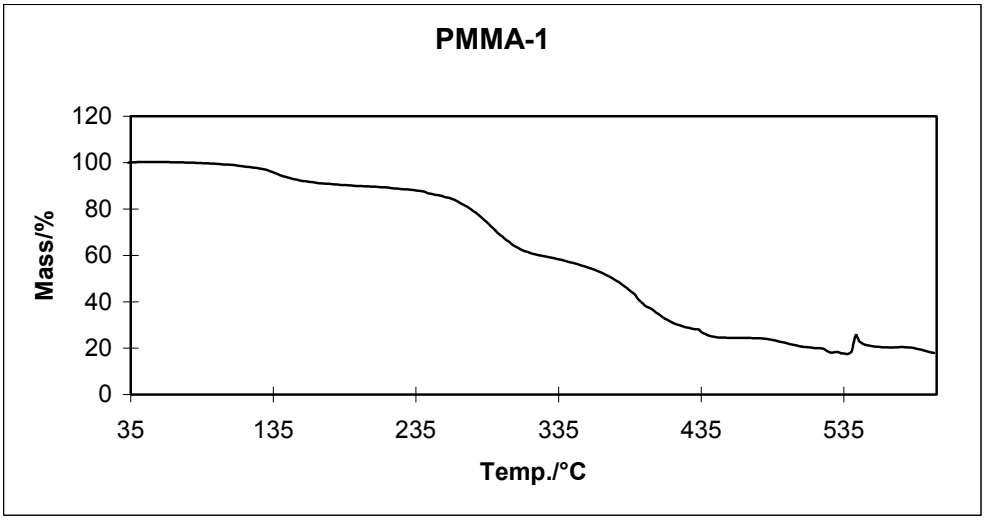

Figure 3.6. TG analysis of poly (methyl methacrylate)-1 (PS-1)

3.2.5.3. Differential Scanning Calorimetry

Differential Scanning Calorimetry (DSC) is the most widely used thermal analysis method for the polymeric material studies. It gives important information about the softening or glass transition temperatures (Tg), melting temperatures, heats of melting, and crystallization behaviors of the materials.[40] A broad crystal-melting peak is the indication of a broad molecular weight distribution, which is a unique polymer property. The Tg gives information about the softness or hardness of the polymer. Hardness is also directly proportional with crystallinity degree. Higher crystallinity means higher stability of the material so the response to external treatments will be slower in turn. Then the more crystalline is a material the lower solubility or a slower dissolution pattern is expected.

Previously conducted TGA/DTA analysis showed that maximum temperature of 300 °C is enough to observe needed phase changes of materials on heating. The experiments are run from –10 °C in order to be sure that no change is missed at low temperatures. In this way, system's initial fluctuations are also limited to low temperatures making available to observe the desired range more accurately.

Heating range was (-10 °C – 300 °C). Heating rate was 10 °C/min, a low rate analysis to guarantee better separation of any close peaks. Glass transition, melting,

crystallization and decomposition trends of the synthesized oligomers were determined. Cooling of the system is achieved by liquid nitrogen. The atmosphere is N_2 gas/N_2 gas during heating and N_2 gas/liqN_2 during cooling. Each time the atmosphere is changed, isothermal step is applied for at least 5 minutes in order to allow the system reach equilibrium and prevent the sudden fluctuations effect the measurement.

3.2.5.3.1. Series I

Glass transition temperatures were observed in the 5 °C - 100 °C temperature range for all oligomer samples. PHBA-1 and PDAM-1 have the lowest Tg transitions at 10 °C. PAM-1 and PAN-1 Tg transitions are both approximately around 45 °C. PMMA-1 and PS-1 show Tg transitions at 60 °C and 70 °C, respectively and are the most brittle materials among all. PC-1 transition peak is at 30 °C. The Tg transition results (giving information about material brittleness) are consistent with the physical appearance of the materials.

PMMA-1 and PAM-1 gave broad decomposition peaks at 290 °C, which is a consistent result when their chemical structure similarities are taken into account.

3.2.5.3.2. Series II

Glass transition temperatures were observed as follows, PMMA-2: 60 °C, PS: 70 °C, PAN-2: 50 °C, PAM-2: 60 °C, PHBA-2: 15 °C, PDAM-2: 15 C°, PC-2: 50 C°, respectively. Again consistence with the materials' physical appearances is observed.

Decomposition peaks were observed for the following oligomers: PMMA-2: 290 C°, PAM-2: 255 C°, PHBA-2: 290 C°, PDAM-2: 285 C°, PC-2: 255 C°, respectively. Table 3.4 compares the transitions observed for the materials of Series II and I.

Table 3.4. Tg transition temperatures of oligomers

Oligomers	Tg transition temperatures (° C)	
	Series I	Series II
PMMA	60	60
PS	70	70
PAN	45	50
PAM	45	60
PDAM	10	15
PHBA	10	15
PC	30	50

3.2.5.4. Nuclear Magnetic Resonance Analyses: Proton NMR

NMR is one of the most important analytical methods available to an organic chemist. It gives information on each type of hydrogen atom, carbon atom, fluorine atom, and etc. depending on the type of the applied NMR method (proton, carbon, fluorine, and etc.).[32] In this way, and with the help of other analytical methods it is possible to obtain important information such as structures of unknowns, conversion degree of a specific reaction, and even molecular weight determination for polymers.

Proton NMR of the oligomers of Series I and II were obtained. Most information was gathered from the proton NMR spectra of the materials.

3.2.5.4.1. Series I

The molecular weight determination, repeating unit of monomers, and type of block formation was determined. The peak observed at δ 4.0-4.2 is the peak coming from the Fluoroinitiator A and corresponds to (t, $4H$,-CF_2-CH_2-OOC-). In this way the integral calculations are performed and monomer/initiator ratios are obtained. For a unit initiator, calculated monomer number gives the repeating unit *n*.

Vinyl group peak detection in the δ 4,5-7 region[42] in the spectra of some of the oligomers accounts for polymerization termination by disproportionation mechanism. Generally acrylic monomers are known to terminate by a combination mechanism and thus

reactions result in tri-block type macromolecule products. However, if the termination occurs by a disproportionation mechanism, the final product is a di-block type macromolecule.[43] In the resulting spectra, the contribution of disproportionation mechanism terminated products is neglected, since vinylic peak integral is very low compared to other peaks. The product co-oligomers are mainly composed of tri-blocks. All NMR spectra are placed in Appendix A.

3.2.5.4.2. Series II

Again, the molecular weight determination, repeating unit of monomers, and type of block formation was determined. The peak observed at δ 4.6-4.65 is the peak coming from the Fluoroinitiator B and corresponds to (t, 4 H, $-CF_2-CH_2-\underline{CH_2}-OOC-$). The integral calculations are performed and monomer/initiator ratios are obtained. Again the contribution of disproportionation mechanism terminated products is neglected. Figures 3.7 and 3.8 illustrate the two mechanisms of termination reactions. All NMR spectra are placed in Appendix B.

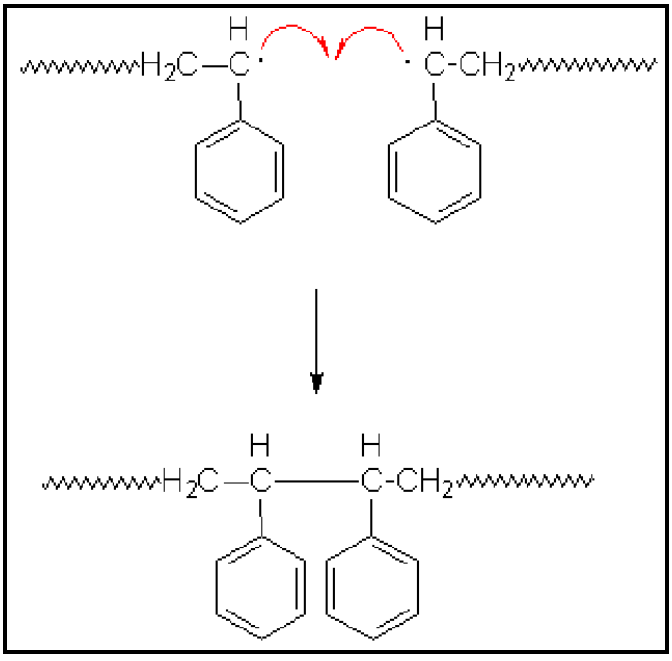

Figure 3.7. Termination by combination

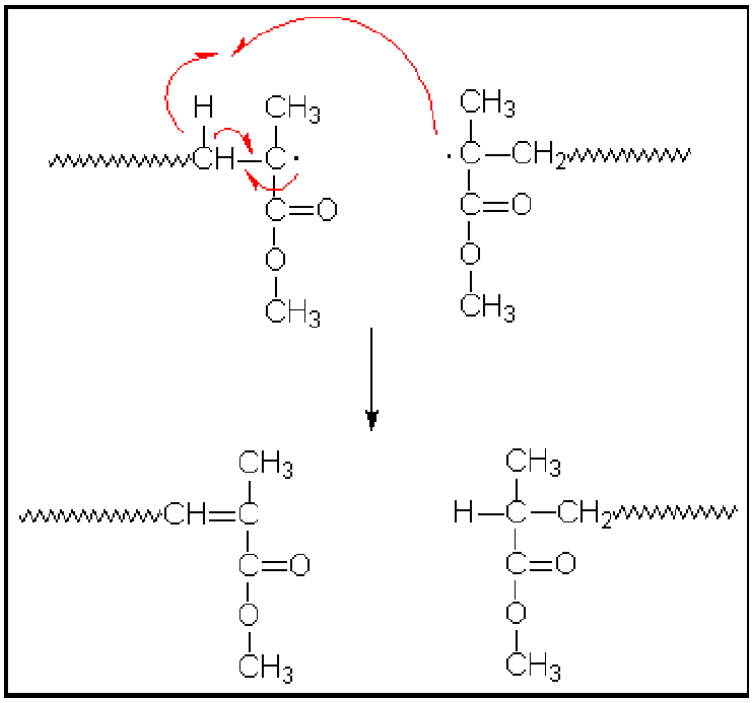

Figure 3.8. Termination by disproportionation

Tables 3.5 and 3.6 display the calculated monomer repeating units and corresponding molecular weights (Mw) for the oligomers of Sets I and II, and in the same time allow the comparison with their $scCO_2$ solubility efficiencies.

Table 3.5. Molecular weight, number of monomer repeating units, and supercritical solubility compared for Series I

Oligomer	**Molecular Weight (MW) (g/mol)**	**Number of Monomer Repeating Units (*n*)**	**Solubility**
PAM-1	1484	8	Readily soluble
PDAM-1	2274	6	Readily soluble
PC-1	2844	8	High solubility
PHBA-1	2988	12	High solubility
PAN-1	2280	12	Moderate solubility
PMMA-1	5600	38	Moderate solubility
PS-1	2300	10	Not soluble

Table 3.6. Molecular weigh, number of monomer repeating units, and supercritical solubility compared for Series II

Oligomer	Molecular Weight (MW) (g/mol)	Number of Monomer Repeating Units (*n*)	Solubility
PAM-2	1794	10	Readily soluble
PC-2	1736	4	Readily soluble
PHBA-2	1520	4	Readily soluble
PDAM-2	1958	6	High solubility
PAN-2	1898	18	High solubility
PMMA-2	2144	12	High solubility
PS-2	1776	8	Low Solubility

3.3. Results and Discussion

3.3.1. Series I

The thermal analysis results of Series I oligomers are highly consistent with the CO_2 solubility observations. PS-I is highly stable as indicated by its high melting and high Tg points. It does not dissolve in $scCO_2$. The solubility efficiencies of other oligomers vary from moderate to highly soluble accordingly with their thermal behaviors. The most soluble and thermally least stable oligomer is PDAM-I. The T*g* points are in the 5 ° C-100 ° C temperature range. The materials having higher Tg transitions are more rigid in physical appearance when compared with the ones having lower Tg transitions. For the Series II materials slight increase in Tg transitions is observed. As stated previously, fluorine atom is a big sized atom and its presence adds bulkiness to the chain, which in turn decreases the

chain mobility of the material.[44] The fluorine atom is too large to allow a planar zigzag structure and the result is added rigidity on the oligomer.[45]

The molecular weight determination is mainly supported by NMR analyses, which show that the repeating unit is dramatically higher for smaller sized monomers. This result is reasonable in the means of functional group availability to the reactive sides. The smaller sized monomers are less sterically hindered and react at higher amounts. The molecular weights of all oligomers vary in the 1484-5600 g/mol range, the lowest being PAM-1: 1484 g/mol and the highest being PMMA-1: 5600 g/mol. The main effect on solubility is introduced by intermolecular interactions taking place between the oligomer and the supercritical fluid. P1-2 is the only monomer having an aromatic group as the side chain. Other oligomers' repeating units are of acrylic type or/and contain etheric oxygen atoms that can interact positively with the supercritical phase or do not complicate fluorine side chains' interactions with the supercritical phase. Then it can be concluded that aromatic groups on the chain interact in a negative manner in means of CO_2 solubility.

The most supercritical CO_2 soluble oligomers are PAM-1 and PDAM-1. PAM-1 is both acrylic type and also has smaller sized repeating units compared to other acrylic type oligomers. When compared with PAM-1, PDAM-1 has larger sized repeating units, but its side chains present on the repeating unit are long and flexible chains, which is a property that allows efficient alignment of these chains with each other and decreases sterical hindrance caused due to interactions with side fluorinated chains that are in turn freer to move. After PAM-1 and PDAM-1, PHBA-1 and PC-1 follow with high solubility efficiencies. PHBA-1 and PC-1 have similar chemical structures to PDAM-1 and they also have long linear side chains, but when compared to PDAM-1, they have higher repeating unit numbers. This accounts for their lower solubility efficiencies compared to PDAM-1. PAN-1, and PMMA-1 follow these with moderate solubility efficiencies. PAN-1's repeating groups are small and are of acrylic type, but these molecules lack the oxygen that acts as a Lewis base in the interactions with the supercritical phase, which is the reason for lower solubility. PMMA-1 on the other hand, is both acrylic, its repeating unit side chains are small compared to PC-1, PHBA-1, and PDAM-1 ones, and contain the critic etheric oxygen. Then its lower solubility compared to PC-1, PDAM-1, and PHBA-1 is reasoned due to the lack of long linear side chain present on the repeating unit. This proves that this

linear chain adds positively to the interactions with the supercritical phase. All of these results are consistent with the theoretical studies conducted previously by Baysal's group.

3.3.2. Series II

Thermal results and $scCO_2$ solubility observations are similarly consistent with each other as in the experiments carried out with Series I. Tg values are over the room temperature again. PS-II is the most stable oligomer and has the lowest solubility. Others show the same arrangement of dissolving performance. However, for all of the oligomers, the solubility is dramatically improved compared to Series I. The result is the evidence for the fluorine segment end group's effect that was discussed previously in the introduction section. The hydrogen present at the end groups is the main reason for this difference. Then selection of the proper initiator with an appropriate end group is of real importance to achieve aimed results.

The molecular weight determination is again mainly supported by NMR analysis, which as stated previously, shows that the repeating unit is dramatically higher for smaller sized monomers. This behavior is attributed to degree of functional group availability to the reactive sides. The molecular weights of all oligomers vary approximately in the same range, form lowest being PHBA-2 with 1520g/mol to highest being PMMA-2 with 2144g/mol. Again the main effect on solubility efficiency is introduced by intermolecular interactions taking place between the oligomer and the supercritical fluid. PS-2 has the lowest solubility, which was attributed previously to the aromaticity present on its repeating hydrocarbon units. As in Series I, the most super critical CO_2 soluble oligomer is PAM-2 because it is both acrylic type and also has smaller sized repeating units compared to other acrylic type oligomers. After come PHBA-2 and PC-2. Both have ester groups, but the repeating units are larger than the ones of PAM-2. Yet their side chains present on the repeating unit are long and flexible chains, which as explained previously, is a property that allows efficient alignment of these chains with each other and decreases sterical hindrance caused due to interactions with side fluorinated chains that are in turn freer to move. PDAM-2, PAN-2, and PMMA-2 follow these with sufficiently high solubility efficiencies. Yet, these are not totally soluble. For PDAM-2 the lower solubility efficiency may be the

result of its higher number of repeating units when compared with PHBA-2 and PC-2 oligomers. The lower solubility efficiencies of PAN-2 and PMMA-2 can be explained by the same reasoning made for PAN-1 and PMMA-1 of Series I.

CHAPTER 4

CONCLUSIONS AND RECOMMENDATIONS FOR FUTURE STUDIES

4.1. Summary of conclusions

4.1.1. Synthesis of Fluorinated Azo-Initiators

The synthesis of azo-based precursors was developed in order to utilize the obtained materials as radical polymerization initiators in the synthesis of fluorinated oligomers for $scCO_2$ applications. At first, isomer separation of starting material ABCVA was performed. Isomer separation is a step that must not be neglected for high purity and high conversion in the next step of the initiator synthesis. The separation efficiency was mainly confirmed with differential scanning calorimetry (DSC) analysis.

The second initiator was obtained at higher convergence and higher purity. The hydrogen atom present at the end carbon atom of the fluorinated alcohol A was assigned as the responsible factor for the lower efficiency obtained in the synthesis of Initiator A. The conversion and purity results were confirmed mainly with infrared spectroscopy (FT-IR) and nuclear magnetic resonance spectroscopy (NMR).

4.1.2. Synthesis of Fluorinated Block Oligomers

The synthesis of fluorinated block oligomers using different commercially available monomers was performed to be utilized as surfactant systems for $scCO_2$ applications. Another important observation was the high stability of PS, which was the effect introduced by the aromatic group present on the chain. Thermal analyses were utilized DSC and simultaneous thermal analyses (STA): DTA and TA.

Important result obtained from the solubility experiments was the realization of the dependence of solubility efficiency on the chemical structure of the oligomer, functional groups present on the chain(s), and repeating unit size. It was experimentally shown that especially acrylic type oligomers having smaller hydrocarbon repeating units and/or having linear side chains on their hydrocarbon segments dissolve more efficiently.

Comparative solubility experiments of the oligomer series (Series-I and Series-II) proved that end group type of the fluorinated segment played the most important role in the efficiency of the surfactant's dissociation through the supercritical environment. The hydrogen atom present at this group decreases solubility efficiency.

As claimed previously, $scCO_2$ promises future developments and advantages as a cheap, environmentally friendly, nontoxic alternative to other organic solvents. However the limitations that are faced with CO_2 utilization are of great importance to the area. This research has shown that with appropriate monomer and precursor selection, it is possible to successfully design considerably efficient surfactants tailored for different needs. The simple dependence of the solubility on the end-group character opens a wide area for the synthesis of different oligomers suitable for different applications. For example, hydrocarbon based surfactants that are utilized widely in several industries, may be enhanced and made CO_2 soluble by the incorporation of fluorinated block segments.

4.2. Recommendations for Future Studies

Small angle neutron scattering (SANS) can give information about the micellar radii of surfactant aggregated formed in $scCO_2$. For detailed analysis of the micelle formation on the micro scale, SANS studies may be carried out and better characterization of the formed micelles may be achieved.[1]

As concluded after the nuclear magnetic resonance studies (NMR) and also as stated by polymerization mechanism theories, the two mechanism types of termination, combination and disproportionation are determinant of the block type formed at the end of the radical reaction. In this work, the main mechanism was combination, since vinylic hydrogen (which is expected to form at the end of a disproportionation mechanism) amount observed in the NMR spectra was very low (almost zero) compared to other hydrogen atom types in the spectra. Thus the effect of disproportionation was simply ignored. It is reasonable that for syntheses requiring high purity, and for applications highly dependent on formed block type, the effect of mechanism of termination is of great importance. Then the clear characterization of the block type formed at the end of the reaction and utilization of controlled reaction conditions for a desired block type is of concern. Another work may be the design and characterization of different block-type fluorinated oligomers. A suitable method dealing with the characterization of formed block types is the laser scattering technique.[59] Together with SANS, the method will also help for improved micelle studies.

Applications of $scCO_2$ are not just limited to polymer-based systems. CO_2 can find usage in water-based systems such as extraction, cleaning processes, phase transfer reactions and catalysis, enzymatic catalysis, etc. Surfactant design is a very wide research area in terms of suitability for the desired application. Fluorination or fluorinated tail addition to commercially known water based surfactants can be another future demanding research alternative.

Another useful study may be the utilization of the synthesized surfactants for several of the previously stated applications in CO_2. These studies are certainly limited by the economic conditions, material, labware and instrument availability, but with careful and intelligent planning and industrial collaboration these problems can be easily faced.

APPENDIX A

PROTON NMR SPECTRA OF SERIES I OLIGOMERS

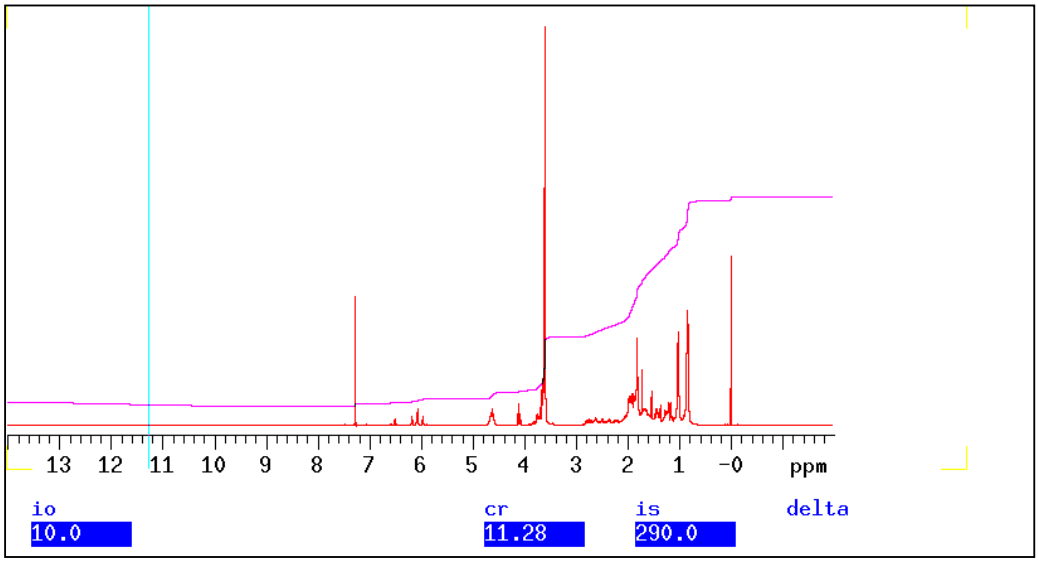

Figure A.1. Proton NMR of PMMA-1

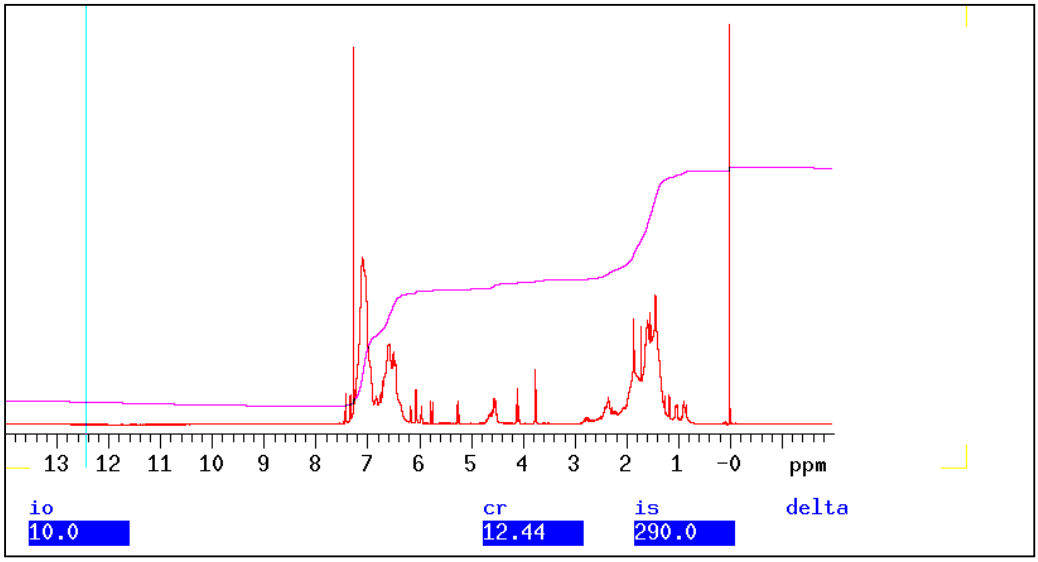

Figure A.2. Proton NMR of PS-1

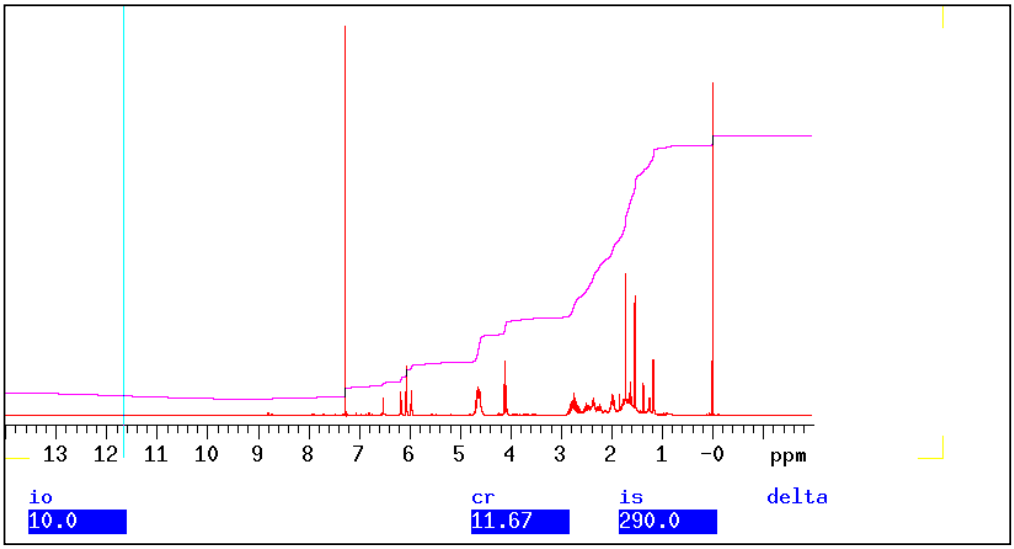

Figure A.3. Proton NMR of PAM-1

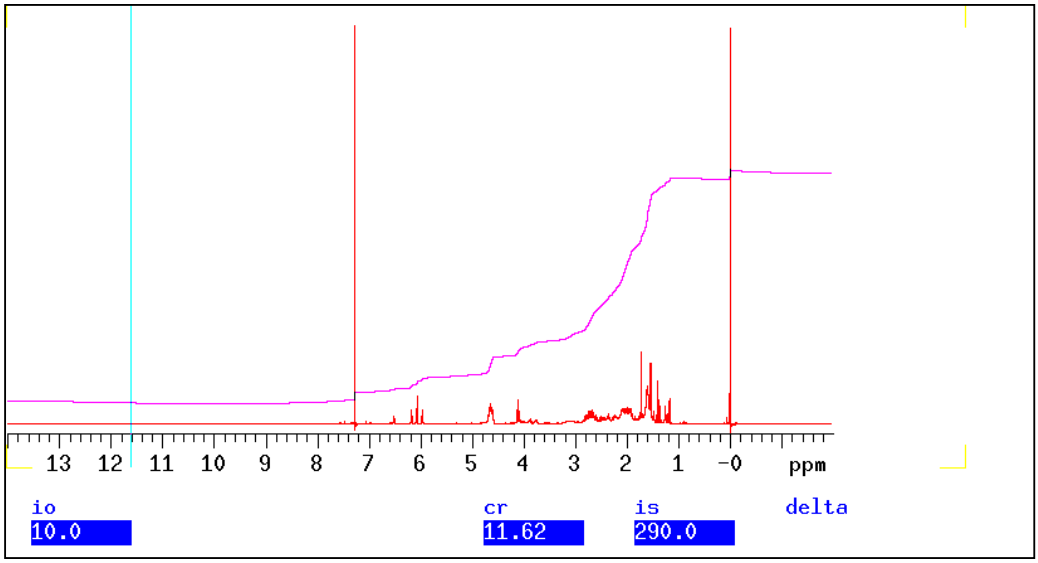

Figure A.4. Proton NMR of PAN-1

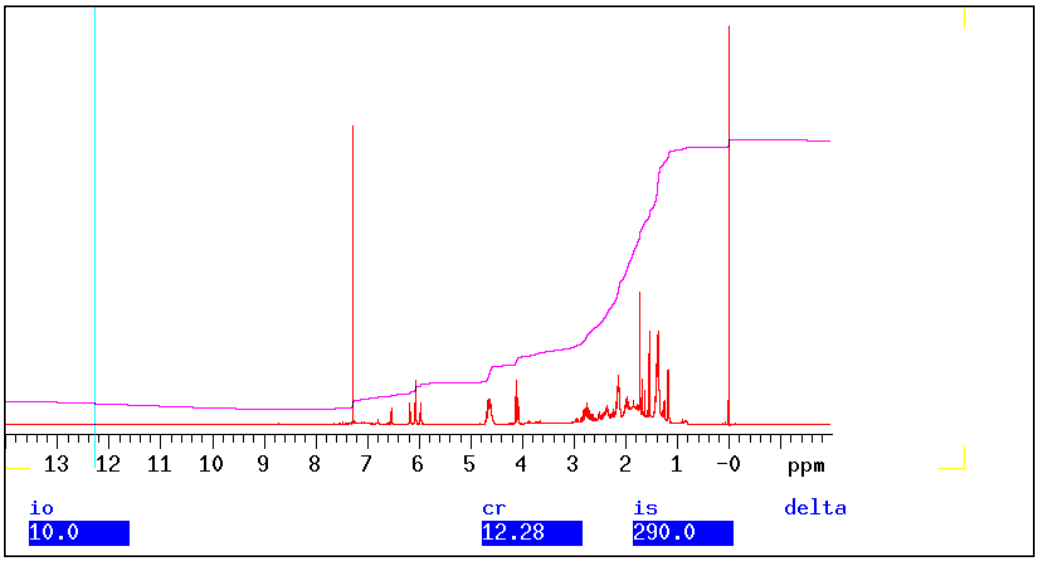

Figure A.5. Proton NMR of PDAM-1

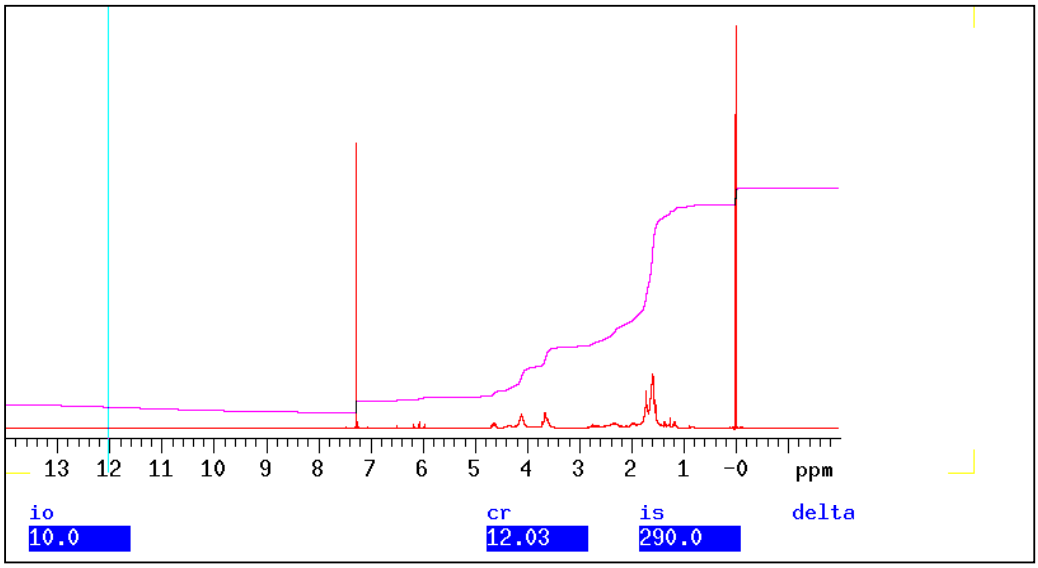

Figure A.6. Proton NMR of PHBA-1

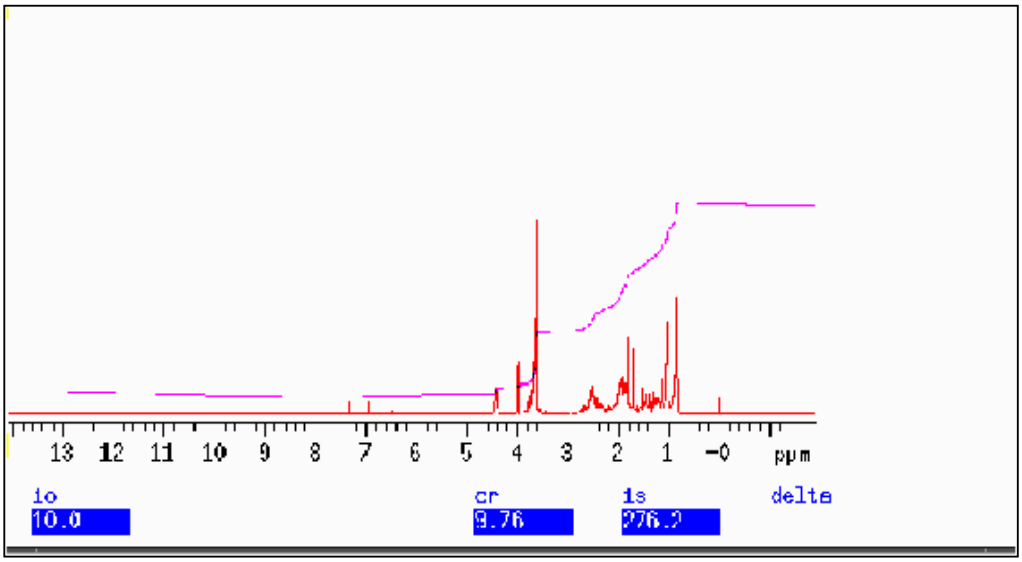

Figure A.7. Proton NMR of PC-1

APPENDIX B

PROTON NMR SPECTRA OF SERIES II OLIGOMERS

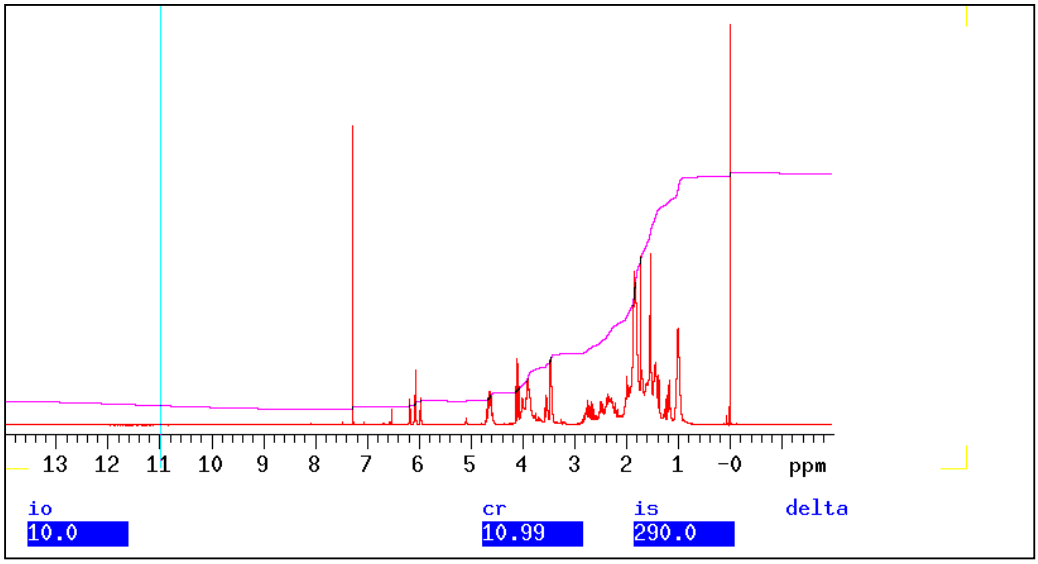

Figure B.1. Proton NMR of PMMA-2

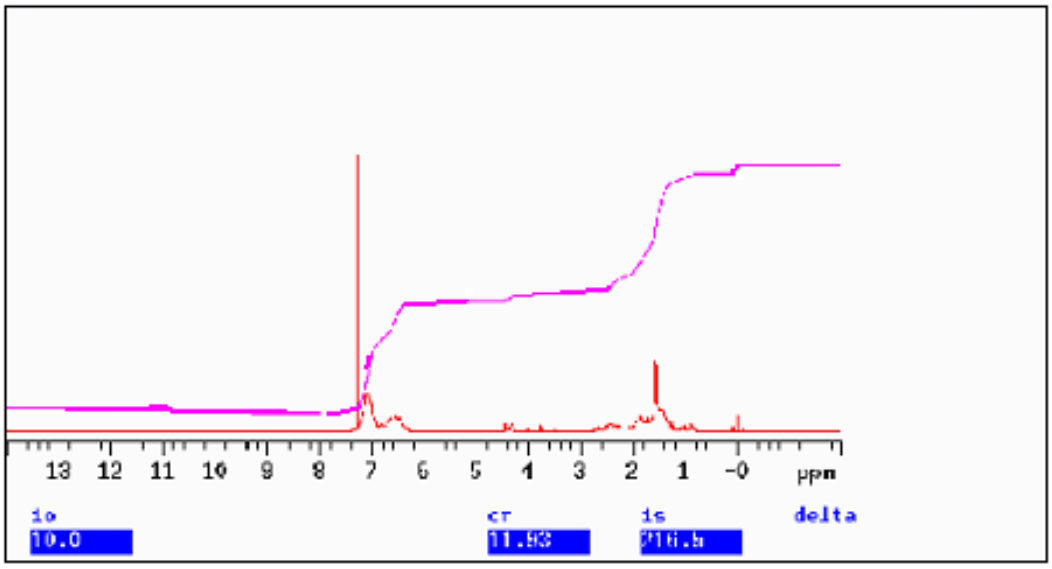

Figure B.2. Proton NMR of PS-2

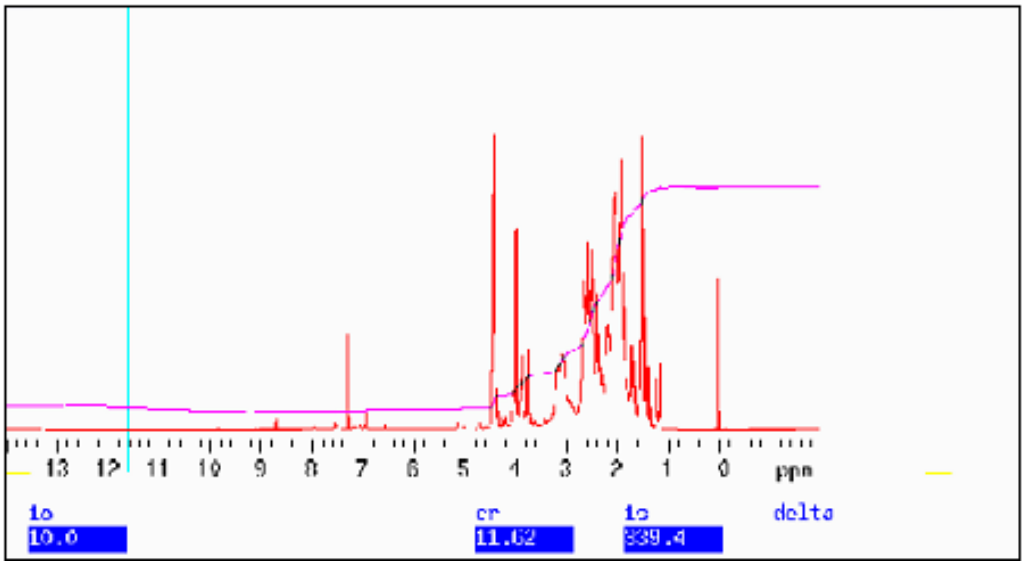

Figure B.3. Proton NMR of PAN-2

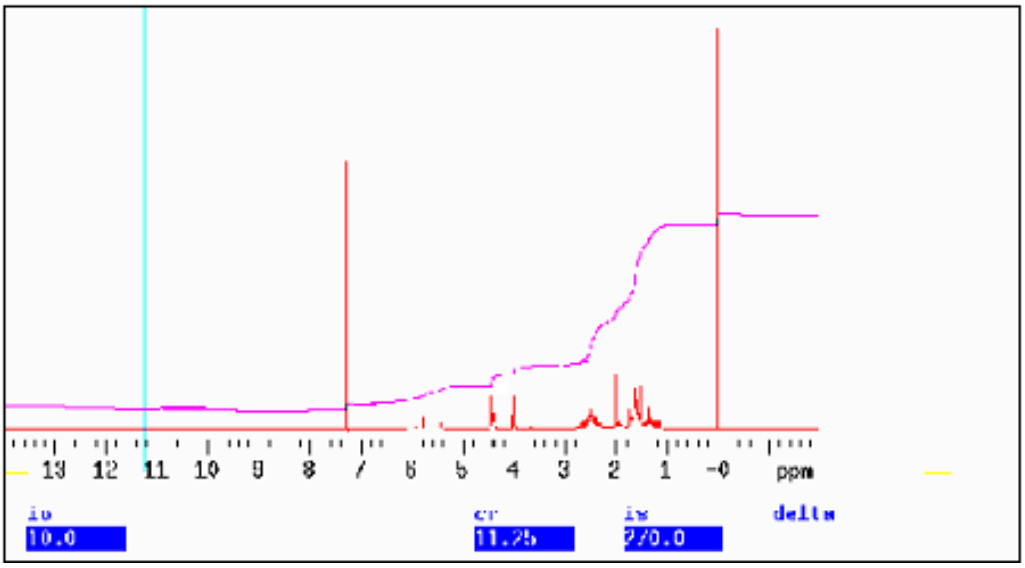

Figure B.4. Proton NMR of PAM-2

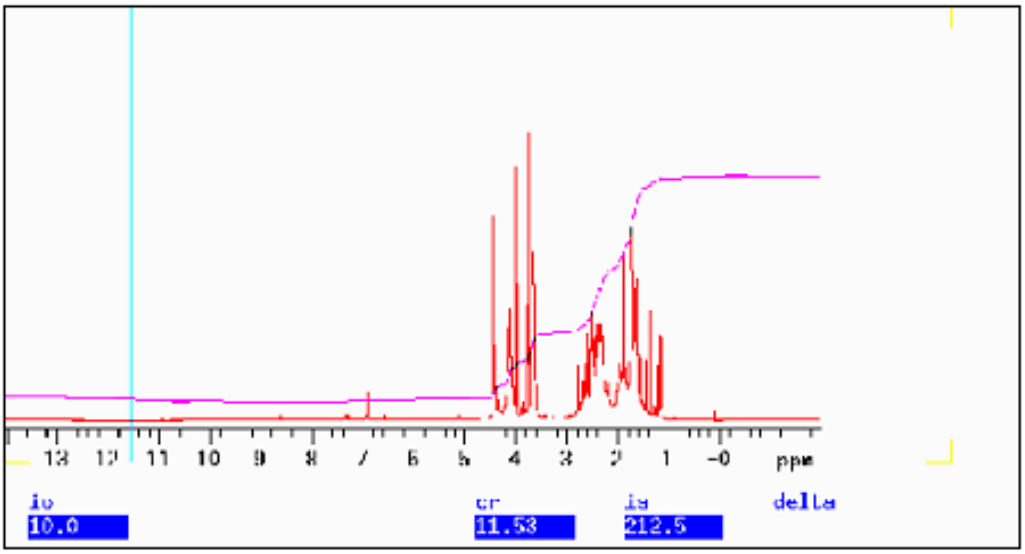

Figure B.5. Proton NMR of PHBA-2

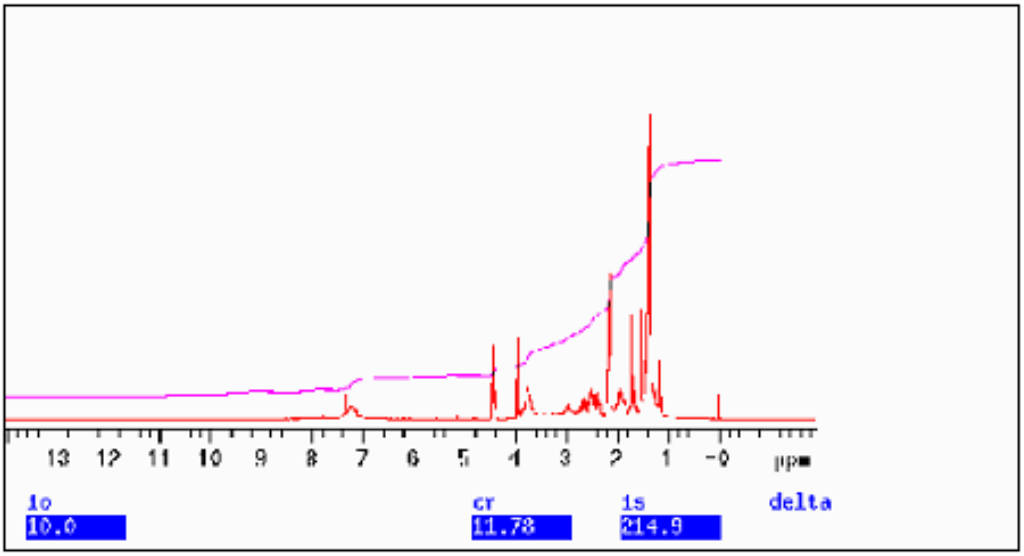

Figure B.6. Proton NMR of PDAM-2

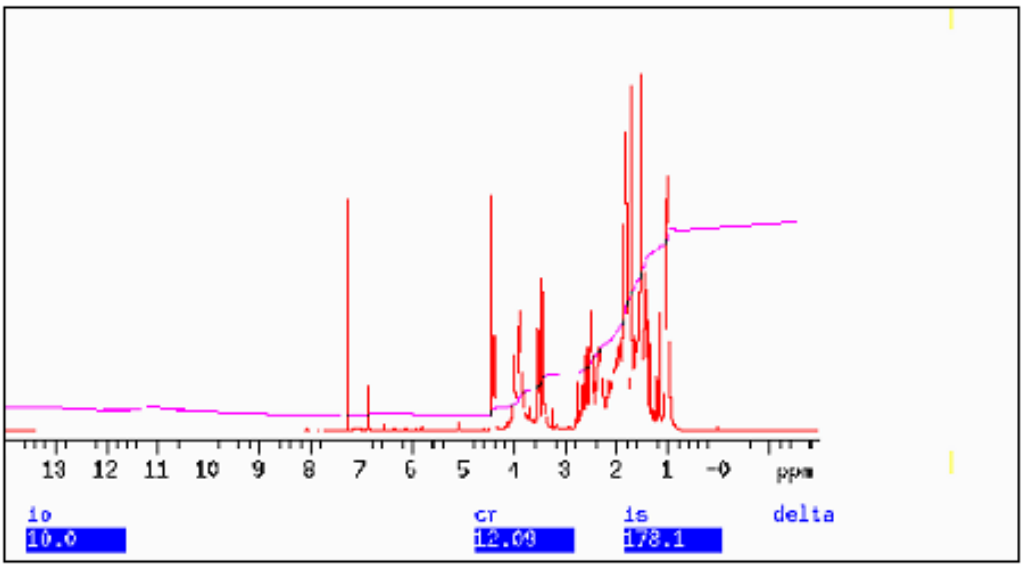

Figure B.7. Proton NMR of PC-2

BIBLIOGRAPHY

[1] Maury, E. Elise. 1995. Heterogeneous Free Radical Polymerizations in Supercritical Carbon Dioxide. Doctoral Thesis, University of North Carolina.

[2] DeSimone, J.M., Maury E.E., Menceloglu Y.Z., McClain J.N., Romack T.J., and J.R. Combes. ‘’Dispersion Polymerizations in Supercritical Carbon Dioxide.’’ *Science* 265 (1994): 356-359.

[3] Jessop, G. Phillip and Walter Leitner. ‘’Phase Behavior and Solubility.’’ In *Chemical Synthesis Using Supercritical Fluids*, ed. Philip G. Jessop and Walter Leitner, 37-53. Weinheim: WILEY-VHC, 1999.

[4] Jessop, G. Phillip and Walter Leitner. ‘’Basic Physical Properties of Supercritical Fluids.’’ In *Chemical Synthesis Using Supercritical Fluids*, ed. Philip G. Jessop and Walter Leitner, 38. Weinheim: WILEY-VHC, 1999.

[5] Jessop, G. Phillip and Walter Leitner. ‘’Temperature and Pressure Effects.’’ *In Chemical Synthesis Using Supercritical Fluids*, ed. Philip G. Jessop and Walter Leitner, 51-53. Weinheim: WILEY-VHC, 1999.

[6] Tsekhanskaya, Y., Iomtev M., and E. Mushkina. ‘’Solubility of Naphthalene on Ethylene and Carbon Dioxide under Pressure.’’ *Russ. J. Phys. Chem*. 9 (1964): 1173-1176.

[7] McHugh, M.A. and V.J. Krukonis. *Supercritical Fluid Extraction*. Boston: Butterworth-Heinemann, 1994.

[8] Menceloğlu, Yusuf. 2002. *Processing in Supercritical Carbon Dioxide*. Report Presentation. Tuzla: Sabancı University.

[9] Kiran, Erdogan, Debenedetti, Pablo G., and Cor J. Peters. ‘’Polymer Prosessing.’’In *Supercritical* Fluids*/Fundamentals and Applications*,ed. Erdogan Kiran, Pablo G. Debenedetti and Cor J. Peters, 27. Dordrecht: NATO Science Series, 1989.

[10] Jessop, G. Phillip and Walter Leitner. ‘Supercritical Fluids as a Media for Chemical Reactions.’’ In *Chemical Synthesis Using Supercritical Fluids*, ed. Philip G. Jessop and Walter Leitner, 6-7. Weinheim: WILEY-VHC, 1999.

[11] Kirmizialtin, Serdal, Menceloglu Yusuf, and Canan Baysal. ‘’New Surfactants Design for CO_2 Applications: Molecular Dynamics Simulations of Fluorocarbon-Hydrocarbon Oligomers.’’ *Journal of Chemistry and Physics* 36 (2003): 1132-1137.

[12] Sarbu, Tralan, Styranec Thomas, and Eric J. Beckman. ‘’Non-Fluorous Polymers with Very High Solubility in Supercritical CO_2 down to Low Pressures.’’ *Nature* 405 (2000): 165-168.

[13] Hoefling, Tracy, Stofesky David, Reid Margaret, Beckman Eric, and Robert M. Enick. ‘’The Incorporation of a Fluorinated Ether Functionality into a Polymer or Surfactant to Enhance CO_2-Solubility.’’ *The Journal of Supercritical Fluids* 5 (1992): 237-241.

[14] Kendall, L. Jonathan, Canelas A. Dorian, Young L. Jennifer, and Joseph M. DeSimone. ‘’Polymerizations in Supercritical Carbon Dioxide.’’ *Chem. Rev.* 99 (1999): 543-563.

[15] Liu, Zhao-Tie and Can Erkey. ‘’Water in Carbon Dioxide Microemulsions with Fluorinated Analogues of AOT.’’ *Langmuir* 17 (2000): 274-277.

[16] Sigma-Aldrich Co. *Biological Detergent Theory and Application*. Available from http://www.sigmaaldrich.com/Area_of_Interest/Biochemicals___Reagents/Biological_Detergents/Detergent_Theory.html. Accessed 19 July 2003.

[17] Jan C.T. Kwak. 1998. ‘’Solubilisation.’’ In *Polymer-Surfactant Systems*, ed. Jan C.T. Kwak. 77: 27-28. New York: Marcel Dekker, Inc.

[18] Triolo F., Triolo A., Celso F. Lo, Donato D. I., and R. Triolo ‘’Dilute and Semi Dilute Solutions of Block Copolymers in Water, Near-critical and Super-Critical CO_2: A Small Angle Scattering Study of the Monomer–Aggregate Transition.’’ *Physica A* 304 (2002): 135-144.

[19] Lisal, Martin, Hall K. Carol, Gubbins E. Keith, and Athanassios Z. Panagiotopoulos. ‘’Micellar Behavior in Supercritical Solvent-Surfactant Systems From Lattice Monte Carlo Simulations.’’ *Fluid Phase Equilibria* (2002): 194-197, 233-247.

[20] Hoefling T.A., Enick R. M., and E. J. Beckman. ‘’Microemulsions in Near-critical and Supercritical CO_2.’’ *Journal of Physical Chemistry* 95 (1991): 7127-7129.

[21] Harrison K., Goveas J., and K. P. Johnston. ‘’Water-in-carbondioxide Microemulsions With Fluorocarbon-Hydrocarbon Hybrid Surfactant.’’ *Langmuir* 10 (1994): 3536–3541.

[22] Clarke, M.J., Harrison K.L., Johnson K.P., and S.M. Howdle. ‘’Water in Supercritical Carbon Dioxide Microemulsions: Spectroscopic Investigation of a New Environment For Aqueous Inorganic Chemistry.’’ *Journal of American Chemical Society* 119 (1997): 6399–6406.

[23] Fremgen, D.E., Gerald R.E., Smotkin E.S., Klingler R.J., and J.W. Rathke. ‘’Microemulsions of Water in Supercritical Carbon Dioxide: An in-situ NMR Investigation of Micelle Formation and Structure.’’ *Journal of Supercritical Fluids* 19 (2001): 287-298.

[24] Lee, C.T., Bhargava P., and K.P. Johnston. ‘’Percolation in Concentrated Water-in-Carbon Dioxide Microemulsions.’’ *Journal of Physical Chemistry* 104 (2000): 4448-4456.

[25] Eastoe, Julian, Paul Alison, and Adrian Downer. ‘’Effects of Fluorocarbon Surfactant Chain Structure on Stability of Water-in_Carbon Dioxide Microemulsions: Links Between Aqueous Surface Tension and Microemulsion Stability.’’ *Langmur* 18 (2002): 3014-3017.

[26] Eastoe, Julian, Dupond Audrey, and David C. Steytler. ‘’Fluorinated Surfactants in Supercritical CO_2.’’ *Current Opinion in Colloid and Interface Science* 8 (2003): 267-273.

[27] Bruice, Paula Yurkanis. ‘’Conformations of Alkenes.’’ In *Organic Chemistry*, ed. Paula Yurkanis Bruice, 2nd Ed: 89-93. Englewood Cliffs: Prentice-Hall, 1998.

[28] Sheppard, Chester Sheppard and Ronald Edward McClay. United States Patent 19-4101522.

[29] Bruice, Paula Yurkanis. ‘Synthesis of Carboxylic Acid Derivatives.’’ In *Organic Chemistry*, ed. Paula Yurkanis Bruice, 2nd Ed: 89-93. Englewood Cliffs: Prentice-Hall, 1998.

[30] Sheppard, Chester Sheppard and Ronald Edward McClay. United States Patent 19-4101522.

[31] Palvia, L. Donald, Lampman M. Gary, and George S. Kriz, Jr. ‘’Infrared Spectroscopy.’’ In *Introduction to spectroscopy: A guide for students of organic chemistry*, 28-73. Phyladelphia: International Thomson Publishing, 1997.

[32] Palvia, L. Donald, Lampman M. Gary, and George S. Kriz, Jr. ‘Nuclear Magnetic Resonans Spectroscopy.’’ In *Introduction to spectroscopy: A guide for students of organic chemistry*, 81-170. Phyladelphia: International Thomson Publishing, 1997.

[33] Macomber, Roger S. ‘’Chemical Shift Correlations for ^{13}C and Other Elements.’’ In *A Complete Introduction to NMR Spectroscopy*, 100. Canada: John Wiley & Sons, Inc, 1997.

[34] Tsang, W. *Energetics of Free Radicals*, ed.A. Greenberg and J. Liebman. New York: Blackie Academic and Professional, 1996.

[35] Haines, P.J. ‘’Kinetics of Solid-state Reactions.’’ In *Thermal Analysis and Calorimetry*, ed. P.J. Haines, 42-50. Cambridge: The Royal Society of Chemistry, 2002.

[36] Bruice, Paula Yurkanis. ‘Boiling Points.’’ In *Organic Chemistry*, ed. Paula Yurkanis Bruice, 2nd Ed: 83843. Englewood Cliffs: Prentice-Hall, 1998.

[37] Bessie, J. Marie, Boutevin Bernard, and Oliver Loubet. ‘’Synthése et caracterisation d'amorceurs azoiques fluorés: Application a l'étude de la reaction de terminaison de chaine lors de la polymérisation radicalaire du styrene.’’ *European Polymer Journal* 31 (1995): 573-580.

[38] Speyer, F. Robert. ‘’Differential Thermal Analysis.’’ In *Thermal Analysis of Materials*, 35-85. New York: Marcel Dekker, Inc,1994.

[39] Speyer, F. Robert. ‘’Differential Thermal Analysis.’’ In *Thermal Analysis of Materials*, 35-85. New York: Marcel Dekker, Inc,1994.

[40] Haines, P.J. ‘Differential Thermal Analysis and Differential Scanning Calorimetry.’’ In *Thermal Analysis and Calorimetry*, ed. P.J. Haines, 55-92. Cambridge: The Royal Society of Chemistry, 2002.

[41] Kaisersberger, E., Knappe S., Möhler H., and S. Rahner. 1994. *TA for Polymer Engineering: DSC, TG, DMA, TMA*. Selb: NETZSCH, 1994.

[42] Haines, P.J. ‘Polymer Stability and Charcoal Production.’’ In *Thermal Analysis and Calorimetry*, ed. P.J. Haines, 33-37. Cambridge: The Royal Society of Chemistry, 2002.

[43] Ravve, A. *Principles of polymer chemistry*. New York: Kluwer Academic/Plenum Publishers, 2002.

[44] W. James Feast, W. James, Gimeno Miquel, and Ezat Khosravi. ‘’Approaches to highly polar polymers with low glass transition temperatures. 1.Fluorinated polymers via combination of ring-opening metathesis polymerization and hydrogenation.’’ *Polymer* 44 (2003): 6111-6121.

[45] Drobny, Jiri George. ‘’Crystallinity and Melting Behavior.’’ In *Technology of Fluoropolymers*, 26-27. Florida: CRC Press, 2001.